International Journal of Modern Physics B, Vol. 10, No. 10 (1996) 1111–1151

ON SELF-ORGANIZED CRITICALITY AND SYNCHRONIZATION IN LATTICE MODELS OF COUPLED DYNAMICAL SYSTEMS

CONRAD J. PÉREZ*, ÁLVARO CORRAL, ALBERT DÍAZ-GUILERA
Departament de Física Fonamental, Universitat de Barcelona
Diagonal 647, 08028 Barcelona, Spain

KIM CHRISTENSEN
Department of Physics, University of Oslo, P.O. Box 1048
Blindern, N-0316 Oslo 3, Norway

ALEX ARENAS
Departament d'Enginyeria Informàtica, Universitat Rovira i Virgili
Carretera Salou s/n, E-43006 Tarragona, Spain

Received 1 November 1995

Lattice models of coupled dynamical systems lead to a variety of complex behaviors. Between the individual motion of independent units and the collective behavior of members of a population evolving synchronously, there exist more complicated attractors. In some cases, these states are identified with self-organized critical phenomena. In other situations, they are identified with clusterization or phase-locking. The conditions leading to such different behaviors in models of integrate-and-fire oscillators and stick-slip processes are reviewed.

1. Introduction

In nature, there are many examples of systems with complex collective behavior. There is a big effort to identify and understand the underlying mechanisms leading to such behavior, but it is difficult to find general rules which could give, *a priori*, information about spatio-temporal complexity. The analysis of the time evolution of the magnitudes which describe an isolated dynamical system is a first step. However, the features of a big system consisting of a large number of individual units (where each unit is a dynamical system itself) interacting according to a given criterion, can be very difficult to determine, even if all the units are identical. The nature of the interaction between units, the type of boundary conditions, and the absence or existence of noise are some ingredients which can change completely the dynamic behavior of a coupled dynamical system.

*E-mail address: conrad@ulyses.ffn.ub.es

One might think that complexity arises when the intrinsic dynamics that govern the temporal behavior of each member of a population as well as the interaction between them follow complicated spatio-temporal rules. Not necessarily. It may arise as a result of the continued local simple interactions between all parts in an extended system. On the other hand, extended systems with complex local features may lead to a "simple" collective behavior. This is observed in some biological systems where after some transient period a regime characterized by a perfect synchrony in the temporal activity of all the members is achieved.

Between the trivial behavior of independent uncorrelated units, which can be analyzed by considering the features of isolated elements, and "simple" collective behaviors such as units evolving in perfect synchrony, there is a wide spectrum of situations. Some of them manifest a large degree of complexity such as systems displaying spatial fractal structures and temporal fractal behavior. Fractal structures appear in a variety of physical systems.[1,2] They are geometrical objects, that look alike on all length scales. The universe consists of clusters of galaxies, organized in clusters of clusters of galaxies and so on. Earthquakes occur on structures of faults ranging from thousands of kilometers to millimeters. Likewise, the coast of Norway contains fjords of all sizes, from very small ones to very big ones. Temporal fractal behavior occurs when the temporal fluctuations in a certain quantity look alike on all time scales. In general, the power spectrum behaves like $1/f^{\varphi}$. When $\varphi \approx 1$ we talk about $1/f$ noise or flicker noise.[3–5] The fluctuations in light intensity of quasars, the flow of the river Nile, and the current flowing through a resistor are but a few examples of systems displaying fluctuations without an intrinsic time scale.

During the last years there has been an increasing interest to understand the mechanisms that lead to other complex behaviors closely related to fractals. In particular, a lot of attention is paid on conservative and nonconservative systems displaying self-organized criticality (SOC). Up to now, SOC has been observed in models of cellular automata, coupled map lattices, and coupled dynamical systems defined on a lattice. It is our purpose in this paper to review the mechanisms as well as the conditions required to observe SOC and the corresponding transition to other collective behaviors.

The paper is organized as follows. In Sec. 2 we review the mechanisms that provoke the occurrence of SOC, in randomly driven as well as in deterministically driven models. In Sec. 3 we analyze different models of oscillators focusing our interest on the conditions required to observe a macroscopic degree of synchronization. We will discuss the effect of both short- and long-range interactions. Section 4 is devoted to investigate the circumstances in which a system develops the behaviors mentioned above, their transitions, and their relations. Finally, in Sec. 5 we present the conclusions of the present work along with the lines we think deserve further investigation in order to deal with more realistic physical problems.

2. Self-Organized Criticality

The ubiquity of spatial fractal structures and temporal fractal behavior observed in physical systems suggests a common underlying dynamical origin. The lack of a characteristic scale is the hallmark of a critical process. In equilibrium, critical processes require a fine-tuning of a relevant physical control parameter such as the temperature or the magnetic field to a critical point. However, nature does not, by itself, provide any fine-tuning of control parameters, and with zero probability it sits at the critical point by accident. Thus it is very unlikely that the wide occurrence of scale-invariance is due to critical processes in equilibrium systems.

Recently, Bak, Tang and Wiesenfeld (BTW) suggested that the frequently observed scale-invariance in nature might be related to the spontaneous organization (spatial complexity) and reorganization (temporal complexity) in slowly driven, dissipative systems.[6,7] Internal mechanisms lead to dissipation (heat generation) and quasi-stationary states are reached in which the average fluxes of energy into and out of the systems are equal. The avalanches that occur when grains are dropped onto a pile have been used to illustrate this idea. When sprinkling grains of sand onto a table, one after the other, a pile builds up. Eventually, the pile ceases to grow and additional grains of sand will ultimately fall off the pile. The attractor of the dynamics is a statistically stationary state with a fluctuating angle of repose. If the slope is too steep, large system spanning avalanches would make the pile to collapse to a more stable configuration. If, on the other hand, the slope is too shallow, only small avalanches would be initiated. The sandpile settles into a state in between with avalanches of all sizes, power-law distributed. This scale invariance suggests that the system is critical in analogy with equilibrium critical phenomena. However, one deals with dynamical nonequilibrium statistical properties and the system evolves naturally to the critical state without any tuning of external control parameters. The criticality is an intrinsic property of the dynamics of the system, and the phenomenon of self-organized criticality may very well provide a connection between the occurrence of fractal structures and $1/f$ noise, as well as being the physical origin of these two phenomena. The earth crust is another example of a self-organized critical system: Along the boundary of tectonic plates, a slow build-up of strain is relaxed through earthquakes of all sizes; the energy-frequency relation of earthquake occurrence, which is related to the Gutenberg–Richter law,[8] is a power-law distribution.

A cellular automaton model for sandpile dynamics[6,7] and other numerical models[9–12] were shown numerically to display SOC. The dynamical rules in the BTW model — also known as the sandpile model — at least intuitively resemble the dynamics of a sandpile. In the sandpile model, each site on a lattice is characterized by an integer variable (local slope), and this variable changes in time due to external perturbations (adding grains of sand) and to interaction between different sites when an avalanche propagates through the system. With very simple rules, the system reaches a state which is characterized by the lack of any characteristic

length or time scale. The simplicity of the model suggests that the phenomenon of SOC could be quite universal: Indeed, it has been scrutinized by a host of researchers in fields spanning statistical mechanics,[13] condensed matter physics,[14,15] geophysics,[10,16] biology,[12] and economics.[17,18]

The notion of self-organized criticality has initiated much experimental work, especially on granular systems. The main object has been to address the question of SOC in real sandpiles. Essentially, two distinct types of experiments have been performed: Rotating a semi-cylindrical drum partially filled with grains at a low, constant velocity,[19–22] or dropping single grains at a low rate on a conical sandpile resting on a circular platform.[23–26] In most of these studies, the flow over the rim of the system (the drop number) was recorded. In a drum experiment, this quantity was found to be nearly periodic in time.[19] Similar behavior was seen for large conical piles: they displayed relaxation oscillations when a system size of 30–40 particle diameters was exceeded.[23] In some of the latter experiments, power-law distributions has been reported for small conical piles. However, recently it has been shown, that these distributions are more likely to be stretched exponentials, that is, a characteristic size for the drop number appears.[27,28] The observed behavior may be attributed to inertial effects, which seem to play an important role in all the experiments.[25,27,29,30] Inertial effects lead to a nonlocal process, whereas in the numerical models only the local geometry determines the dynamics. Furthermore, we notice, that the relationship between the drop number measured in experiments and the avalanche size measured in numerical models is unclear. For an alternative view on the dynamics of granular material see the work by Mehta and Barker[31] which reviews the progress that has been achieved experimentally and theoretically.

In a recent experiment, the internal dissipated energy due to avalanches in a slowly driven one-dimensional ($1D$) rice pile, was recorded[27] and it was shown that the occurrence of SOC depends on details in the grain-level dissipation mechanism. With spherical grains, a stretched-exponential distribution was observed implying a characteristic scale which is inconsistent with SOC. The spherical grains typically accumulated kinetic energy when moving down the slope. However, with more elongated grains, the dynamics was dominated by sliding grains. This induced a higher effective friction which suppressed the inertial effects, and a power-law distribution of avalanche sizes appeared. This provides the first experimental evidence of self-organized critical behavior in slowly driven granular systems.

2.1. *Randomly driven models*

First, we briefly discuss the $1D$ BTW sandpile model. Although the behavior of the $1D$ model is trivial, it illustrates the basic concepts of the more complex behavior displayed by the $2D$ BTW sandpile model.

The $1D$ sandpile model[7] is a cellular automaton where an integer variable h_i gives the height of the pile at site i. We define the local slope z_i at site i as

$$z_i = h_i - h_{i+1} \,. \tag{1}$$

The addition of a grain of sand on a randomly chosen site i ($h_i \to h_i + 1$) results in the following changes in the slopes

$$\begin{aligned} z_i &\to z_i + 1\,, \\ z_{i-1} &\to z_{i-1} - 1\,. \end{aligned} \tag{2}$$

We proceed by dropping grains at random sites until one site reaches a slope which exceeds a critical value, $z_i > z_c$, and the site topples by transferring one grain to its neighboring site on the right, that is,

$$\begin{aligned} z_i &\to z_i - 2\,, \\ z_{i\pm1} &\to z_{i\pm1} + 1\,, \end{aligned} \tag{3}$$

unless at the rightmost site where the sand grains fall off the pile. The neighbors that are affected by the toppling may topple in turn generating a chain reaction or *avalanche*. During the avalanche, no grains are added to the pile thus separating the two time scales involved in the dynamic evolution of the pile, a slow time scale for the addition of the grains and a fast time scale for the relaxation processes. The avalanche stops when the system reaches a stable state with $z_i \leq z_c \ \forall i$ and another grain is added following (2) until a new avalanche is initiated and so on. After a transient period, whose duration depends on the initial conditions, the system reaches a critical state in which $z_i = z_c \ \forall i$. This state is a fixed point of the dynamics, since after any perturbation the system relaxes returning to the stable state; the added grain will tumble down the slope and simply fall off the pile. The fixed point is an attractor for the dynamics, however, this state has no spatial structure, and correlation functions are trivial.

In the $2D$ sandpile model (on a square lattice),[6] an integer $z_{i,j}$ is assigned to each lattice site (i,j), where $i,j = 1,\ldots,L$. The integer $z_{i,j}$ represents an appropriate dynamical variable (e.g. height of a column of sand, mechanical stress, heat, pressure, or energy[6,32]) on site (i,j) in a spatially extended system.

We perturb the system (add sand to it) by choosing at random a position and increasing the dynamical variable with one unit, that is, $z_{i,j} \to z_{i,j} + 1$. Whenever the dynamical variable on site (i,j) exceeds a threshold value $z_{i,j} > z_c$, the site topples,

$$z_{i,j} \to z_{i,j} - 4\,, \tag{4}$$

$$z_{nn} \to z_{nn} + 1\,, \tag{5}$$

where z_{nn} denotes the height at nearest neighboring sites. As a result one or more neighbors may exceed the threshold value in which case they have to relax and an avalanche will propagate through the system. The toppling rule conserves the amount of z-values whenever an interior site topples. Dissipation only occurs when a boundary site topples assuming open boundary conditions (bc).

The $2D$ sandpile will evolve into a statistically stationary state where, on the average, the rate of flow into the system equals the rate of flow out of the system

across the boundary. Whenever the average slope becomes too large, system spanning avalanches can occur, which transfer grains to the boundary. On the other hand, when the average slope is too small, avalanches tend to be small, and the pile builds up. The stationary state is no longer a fixed point as in $1D$ but a complex attractor. Dhar[33] has calculated the exact number of states in the attractor. When $z_c = 3$, only $(3.210\cdots)^{L^2}$ of the 4^{L^2} stable states are allowed. Furthermore, the dynamics which takes the system from one allowed state to another is ergodic in the sense that all the allowed states occur with equal probability.[33]

One way of characterizing the dynamics in a system of linear size L, is to measure the distribution of avalanche sizes defined as the total number of topplings. Let $P(s, L)$ denote the probability of initiating an avalanche of size s in a system of size L. In the stationary state, an added particle will eventually fall off the boundary of the system. The average distance a particle has to flow in order to reach the boundary is proportional to L due to the random deposit. The average avalanche size $\langle s \rangle = \int sP(s, L)\, ds$ must be infinite in the thermodynamic limit $L \to \infty$. Indeed, averaged over a large number of perturbations (after the transient period), the avalanche size distribution is a power law

$$P(s, L) \propto s^{1-\tau} \tag{6}$$

limited only by the size of the system, see Fig. 1(a). From these results the power-law exponent τ is 2.15 ± 0.1. Since the cutoff is a finite size effect, the average avalanche size tends to infinity when $L \to \infty$. A data collapse for different system sizes L is obtained when plotting $L^{\beta} P(s, L)$ or $s^{\tau-1} P(s, L)$ against the rescaled variable s/L^{ν}, see Figs. 1(b–c). Thus we can write

$$P(s, L) = L^{-\beta} F(s/L^{\nu}), \tag{7}$$

or, alternatively,

$$P(s, L) = s^{1-\tau} G(s/L^{\nu}), \tag{8}$$

with $G(x) = x^{\tau-1} F(x)$. The exponent $\beta = \nu(\tau - 1)$, where τ is the power-law exponent and ν a critical index expressing how the cutoff scales with system size. The scaling function F approaches a power law (or, equivalently, G a constant) when $s/L^{\nu} \to 0$ since the avalanche size distribution becomes independent of the system size when $L \to \infty$ and decays very quickly for $s \gg L^{\nu}$.

The BTW relaxation rules (4) and (5) conserve the dynamical variable z except at the boundary. Introducing nonconservative dynamics in the interior of the system will leave the BTW model noncritical. Changing rule (4) to, say, $z_{i,j} \to z_{i,j} - 5$ while (5) remains unchanged, one grain of sand will dissipate for every toppling. In the stationary state, the average rate of dissipation equals the average rate of flow into the system. Thus $\langle s \rangle = 1/P_{z_c}$ where P_{z_c} is the probability of adding a grain to a site with z_c units, thereby initiating an avalanche. This probability will approach a constant value when $L \to \infty$, that is, $\langle s \rangle$ will approach a finite value. Such a system cannot display SOC. The avalanche size distribution decays exponentially

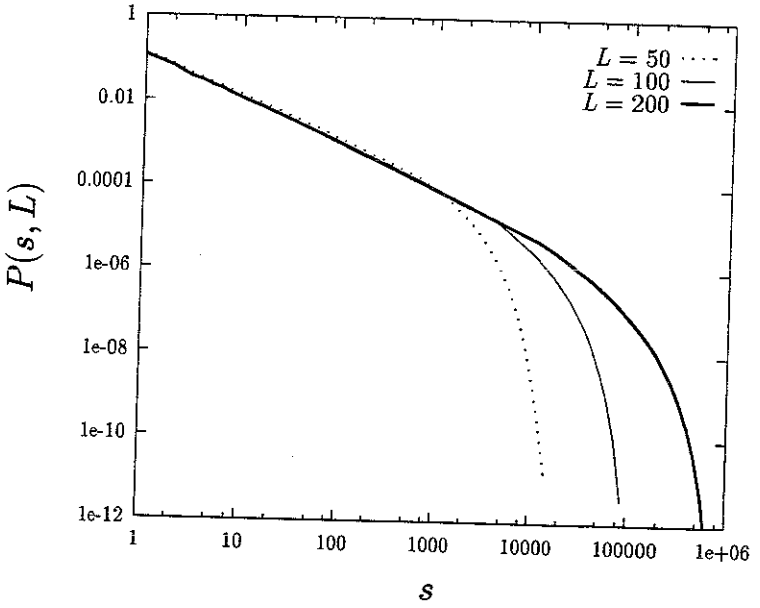

(a)

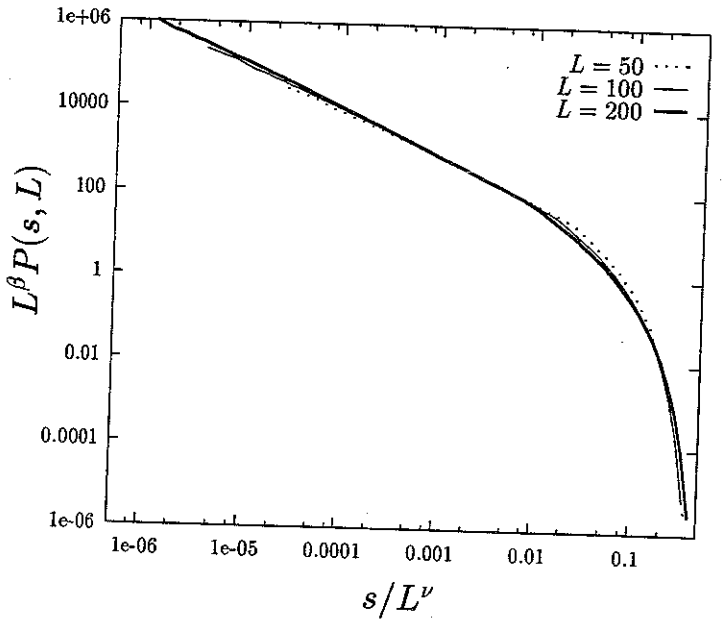

(b)

Fig. 1. The $2D$ Bak, Tang, and Wiesenfeld sandpile model for system sizes $L = 50, 100$, and 200 with open bc. (a) The probability of initiating an avalanche of size s in a system of size L, $P(s, L)$ decreases algebraically with s. The cutoff is a finite-size effect. The displayed distribution functions are averaged over exponentially increasing bins. (b) Using Eq. (7), a reasonable data collapse is obtained with $\tau = 2.15 \pm 0.1$ and $\nu = 2.7 \pm 0.1$. (c) However, the alternative data collapse suggested by Eq. (8) shows the bad scaling of the model for "small" system sizes.

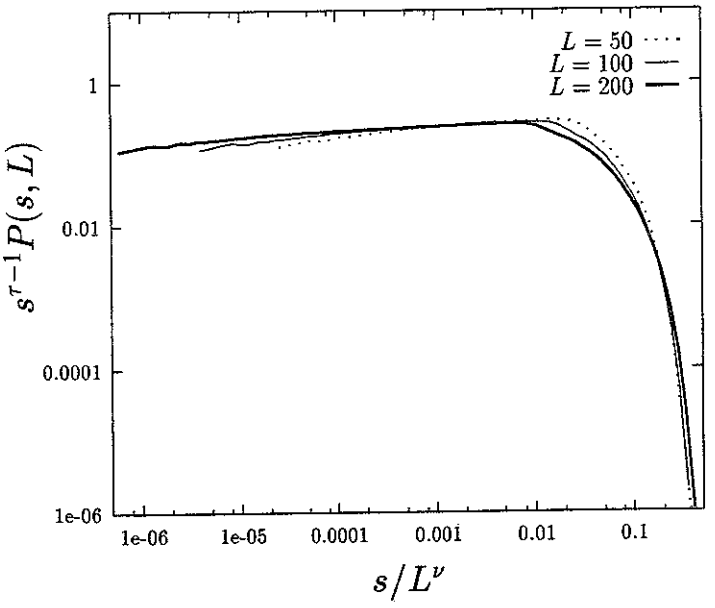

(c)

Fig. 1. (*Continued*)

with a characteristic avalanche size, that does not depend on the system size, and the avalanches are "localized". However, a system with globally conservative but locally nonconservative dynamical rules (changing rule (4) to $z_{i,j} \to z_{i,j} - 4 + \theta$, where $\theta \in \{-3, ..., 3\}$ is an annealed random variable) displays SOC.[34]

Memory effects can be introduced into the BTW model in the sense that a site which has relaxed cannot receive any amount from neighboring sites during the ongoing avalanche. This kind of memory effects makes the dynamics nonconservative and hence destroys the SOC behavior.

In order to model the early experiments on SOC in slowly driven granular piles, inertia effects were included in a BTW-like model.[30] It was observed that when the system size exceeded a certain size, characteristic system spanning avalanches appeared due to the inertia effects in agreement with experiments on real sandpiles.[19,25,29,30] Thus the presence of inertia effects also destroy the SOC behavior.

An apparently different stochastically driven continuous-energy model was introduced by Zhang.[35] In this model, a real number $E_{i,j}$ is assigned to each site (i,j) on a square lattice. The system is perturbed randomly by adding an amount δE to a randomly chosen site, that is, $E_{i,j} \to E_{i,j} + \delta E$. If the value at any site exceeds the threshold value $E_{i,j} > E_c$, the system relaxes according to

$$\begin{aligned} E_{nn} &\to E_{nn} + \varepsilon E_{i,j}\,, \\ E_{i,j} &\to 0\,, \end{aligned} \tag{9}$$

with $\varepsilon = 0.25$. The system is conservative and dissipation occurs only at the boundary, where the number of nearest neighbors is less than 4. The model was studied with $E_c = 1$ and δE chosen uniformly in the interval $[0, 0.5]$,[32,35] in which case it is believed to be in the same universality class as the $2D$ BTW model, that is, the values of critical exponents, such as the power-law exponent τ and scaling index ν, are identical.[36,37]

With $\varepsilon < 0.25$, the dynamics in the Zhang model is nonconservative. When δE is chosen in the range $[0.1, 1]$, the nonconservative relaxation rule introduces a characteristic avalanche size. In this case, the Zhang model is also noncritical in the presence of nonconservation. Furthermore, the introduction of the memory effects mentioned above leads to a characteristic avalanche size inconsistent with the hypothesis of SOC. Similar models have been considered in the context of fracturing.[38] However, additional rules were introduced in order to make the dynamics globally conservative which introduces a kind of inertia effects. Indeed, the general behavior of such systems is the periodic generation of system spanning avalanches coexisting with power-law distributed small avalanches.

The microscopic rules of the lattice models can be written in the form of a set of coupled equations, one for each site. For a continuous version of the stochastically driven BTW model we have[39]

$$E_{i,j}(t+1) = E_{i,j}(t) - \Theta(E_{i,j}(t) - E_c)\, E_c + \sum_{nn} \Theta(E_{nn}(t) - E_c)\, E_c/4 + \eta_{i,j}(t)\,, \quad (10)$$

where $\Theta(x) = 0$ when $x \leq 0$ and $\Theta(x) = 1$ when $x > 0$ is the Heaviside function. The variable t refers to lattice updates. However, in a slowly driven system, the physical time between lattice updates is very short when avalanches are propagating and very long when perturbing the system.[40] The sum takes into account a possible increase in the dynamical variable due to toppling of nearest neighboring sites nn. When an avalanche has come to a halt, a random site is perturbed. The random drive is represented by

$$\eta_{i,j}(t) = \eta\, \delta_{i,n} \delta_{j,m} \prod_{k,l} [1 - \Theta(E_{k,l}(t) - E_c)]\,, \quad (11)$$

n, m being two random integers between 1 and L chosen once for each lattice update, and k, l two indexes running over all the lattice sites. In the original BTW-model $\eta = 1$. The Heaviside function Θ that appears in the noise terms represents the separation of time scales. The models are driven slowly in the sense that no perturbation takes place while avalanches evolve. On the other hand, for the conservative Zhang model, where the toppling variable is reset to zero, the corresponding equations are

$$E_{i,j}(t+1) = [1 - \Theta(E_{i,j}(t) - E_c)]\, E_{i,j}(t) + \sum_{nn} \Theta(E_{nn}(t) - E_c)\, E_{nn}(t)/4 + \eta_{i,j}(t)\,. \quad (12)$$

The noise $\eta_{i,j}(t)$ is again given by (11). In the original Zhang model, η is chosen uniformly in the interval $[0, 0.5]$. In order to deal analytically with these equations,

one usually neglects the Heaviside function in the noise term. This fact creates some difficulties, since the notion of avalanches in such models is not well-defined.[41]

Equations (10) and (12) can be coarse-grained in order to obtain a continuum equation for the effective $E(\mathbf{r},t)$. Using the prescriptions for the temporal derivative and the Laplace operator one gets, after a rescaling of the energy $E - E_c \to E$[42]

$$\frac{\partial E(\mathbf{r},t)}{\partial t} = \alpha\nabla^2[(ZE(\mathbf{r},t) + E_c)\Theta(E(\mathbf{r},t))] + \eta(\mathbf{r},t)\,, \tag{13}$$

where $Z = 1$ for the Zhang model and 0 for the continuous BTW model. The noise $\eta(\mathbf{r},t)$ takes into account the effective external noise as well as the internal noise that appears due to the elimination of internal degrees of freedom.

On the other hand the Θ-function representing the threshold dynamics is modeled as the limit of a smooth function, whereupon dynamical renormalization group calculations can be applied.[36,40] This fact also changes the problem intrinsically. Left to itself, without adding noise, the model would relax to a unique flat ground state with $E(\mathbf{r},t) = 0$. The concept of stable states (or memory) is removed. Some other authors have built nonlinear stochastic differential equations according to the symmetries of the discrete models.[43–45] One should distinguish, however, between these approaches, in which the main goal is to study the "generic scale invariance" by means of dynamical renormalization group theory, and the lattice models.

2.2. *Continuously driven models*

A continuously driven dynamical system was introduced by Olami, Feder, and Christensen (OFC) in the context of earthquake modeling.[10] Though the dynamics of earthquakes is very complex there are two basic components which have to enter a model: (a) earthquakes are generated by the very slow relative motion of tectonic plates, (b) they occur as abrupt rupture events when the fault can no longer sustain the stress, that is, the occurrence is intermittent. Hence, there are two time scales involved in the process; one is related to the stress accumulation while the other, which is orders of magnitude smaller, is associated with the duration of the abrupt releases of stress. A simplified spring-block model introduced by Burridge and Knopoff[46] includes the basic components mentioned above. The model consists of a $2D$ network of blocks interconnected by springs. (For a review of the work of $1D$ Burridge–Knopoff models of earthquake faults, see the work by Carlson, Langer, and Shaw.[16]). Each block is connected to the four nearest neighbors. Additionally, each block is connected to a single rigid driving (tectonic) plate by another set of springs as well as connected frictionally to a fixed rigid (tectonic) plate, see Fig. 2.

Strain is accumulated uniformly across the system as the rigid plates move with a constant relative velocity. When the strain on one of the blocks exceeds the static friction force, the block slips. The released stress is transferred to the neighboring blocks, which in turn may slip, and an earthquake can evolve. This simple picture can be mapped to a coupled map lattice model.[47] A uniformly increasing stress is assigned to each lattice site (i,j). When a block exceeds the threshold stress E_c

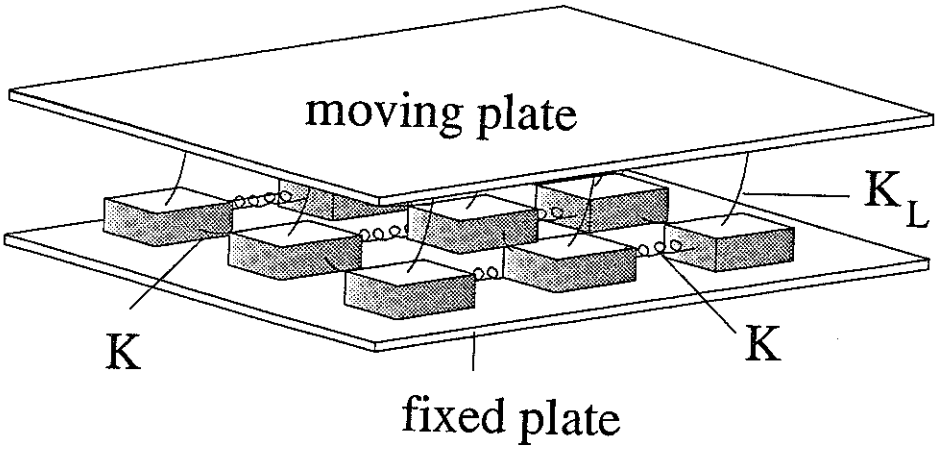

Fig. 2. The $2D$ spring-block model of an earthquake fault. All the blocks are connected to a moving plate by springs with spring constant K_L. The blocks are also connected to the four nearest neighbors through springs of strength K. (After Olami, Feder, and Christensen[10])

it slips. Simple arguments lead to the relaxation rules identical to Eq. (9) with $\varepsilon = K/(4K + K_L)$, K and K_L denoting the spring constants in the model, see Fig. 2. The earthquakes are considered to be instantaneous, that is, the loading of the system stops during an earthquake and the driving recommences when the evolving earthquake has come to a halt. The size of an earthquake is defined as the total number of relaxations.

When $\varepsilon = 0.25$, the model is a continuously driven version of the Zhang model.[a] Apparently, this model has the same power-law exponent τ as the stochastically driven models. However, since $K_L \neq 0$, the generic situation corresponds to the nonconservative case where $\varepsilon < 0.25$.

In Fig. 3(a) we plot the results of a simulation with $\varepsilon = 0.20$ for different system sizes. A reasonably good data collapse is obtained using the finite-size scaling ansatz Eq. (7), see Fig. 3(b). Thus the system is scale invariant; it displays SOC behavior even in the nonconservative case.

When introducing nonconservative relaxation rules into the stochastically driven BTW and Zhang models, the distribution of avalanche sizes decay exponentially with a characteristic avalanche size. The systems are subcritical. Thus the occurrence of criticality in the nonconservative OFC model is very intriguing since it suggests a different mechanism for the generation of the scale invariance. Since the majority of natural phenomena are inherently nonconservative, the SOC behavior

[a]There is also a uniformly driven continuous version of the $2D$ BTW sandpile model.[7] Choosing random initial conditions, this model will be in the same universality class as the stochastically driven integer model. In the continuous model, the fractional part of the dynamical variable takes, in some sense, the role of the random number generator. Note that this model and the OFC model are deterministic. The inherent randomness enters via the initial conditions.

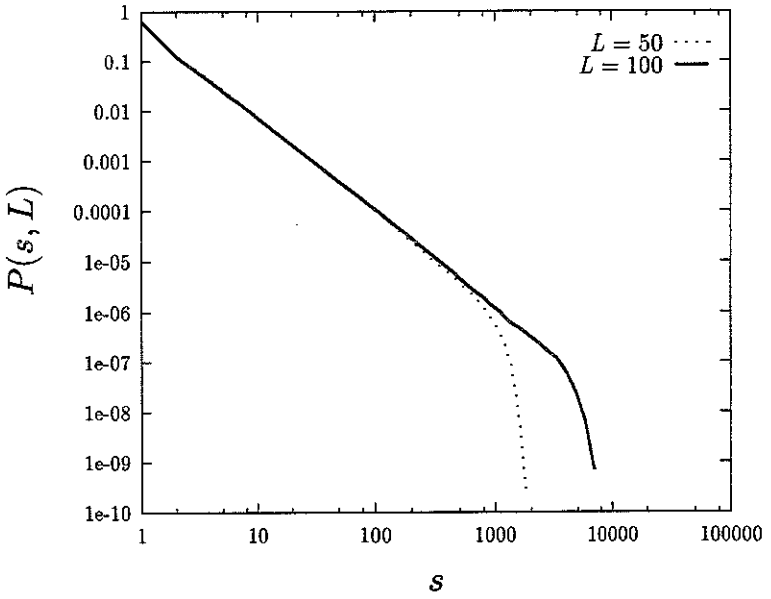

(a)

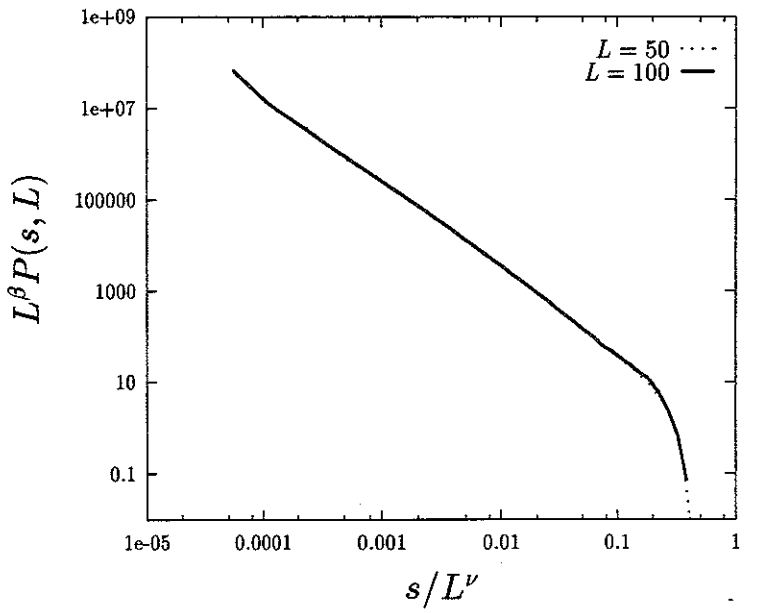

(b)

Fig. 3. (a) The probability density $P(s, L)$ of having an earthquake of size s when $\varepsilon = 0.20$, for the OFC model. The different curves refer to different system sizes $L = 50$, and 100. The cutoff in energy distribution increases with system size L. (b) A finite-size scaling plot using Eq. (7) with $\tau = 2.9 \pm 0.1$ and $\nu = 2.15 \pm 0.1$.[48,49]

of nonconservative systems is probably much more generic than the corresponding behavior of conservative systems.

The microscopic rules for the continuously driven OFC model are given by[39]

$$E_{i,j}(t+1) = [1 - \Theta(E_{i,j}(t) - E_c)]\, E_{i,j}(t) + \varepsilon \sum_{nn} \Theta(E_{nn}(t) - E_c)\, E_{nn}(t) + \eta(t) \quad (14)$$

where

$$\eta(t) = \eta \prod_{k,l} [1 - \Theta(E_{k,l}(t) - E_c)] \quad (15)$$

is a global perturbation. In simulations, one uses $\eta = E_c - E_{\max}(t)$ where $E_{\max}(t)$ is the maximal value of all the dynamical variables in the lattice after the avalanche has come to a halt. To simulate this model a very efficient algorithm has been proposed by Grassberger.[50]

The only difference between the Zhang model and the OFC model is the way of driving. The uniform (global) driving must be a crucial element in driving nonconservative models to criticality.[51] To move continuously between stochastically and uniformly driven systems, one can perturb the system randomly by adding a fixed amount δE to a randomly chosen site (i,j), that is, $E_{i,j} \to E_{i,j} + \delta E$. If the value at any site exceeds the threshold value $E_{i,j} > E_c$, the system relaxes according to Eq. (9). The limit of small δE is the limit of continuous drive. Figure 4 shows the distribution function of avalanche sizes $P(s,L)$ for $\varepsilon = 0.20$ and various values of δE. The avalanches are localized for "large" values of δE. The distribution function is essentially an exponentially decreasing function and no scale invariance is observed when changing the system size. Apparently a phase transition from a localized into a critical system occurs between Fig. 4(c) and 4(d). For "small" values of δE the distribution function approaches a power-law behavior and the cutoff scales with system size, implying that the avalanches are no more localized.

The random drive represents an effective noise given by $\sqrt{\frac{E_c - E_{\max}(t)}{\delta E}}\delta E \propto \sqrt{\delta E}$. Obviously, large noise can destroy spatial correlations in a coupled dynamical system,[b] but the $\delta E \to 0$ represents the weak noise limit where long-range correlations can appear.[51] Analytically, the nonconservation introduces a length scale which in principle one expects to break the scale invariance. Additionally, the continuous driving is difficult to handle analytically. However, an appealing approach would be to treat the OFC model in the limit of random weak noise driving since this is conceptually equivalent to a continuous driving.

[b]This is seen for example in the model discussed by Manna, Kiss, and Kertész,[34] where the dynamical rule destroys the spatial correlations in the BTW model by letting the toppling site $z_{i,j} \to z_{i,j} - 4 + \theta$, where $\theta \in \{-3, \ldots, 3\}$ is an annealed random variable. They obtain $\tau_s = 2.515 \pm 0.02$ in perfect agreement with the analytical result $\tau_s = 5/2$ for models without spatial correlations.[51,52]

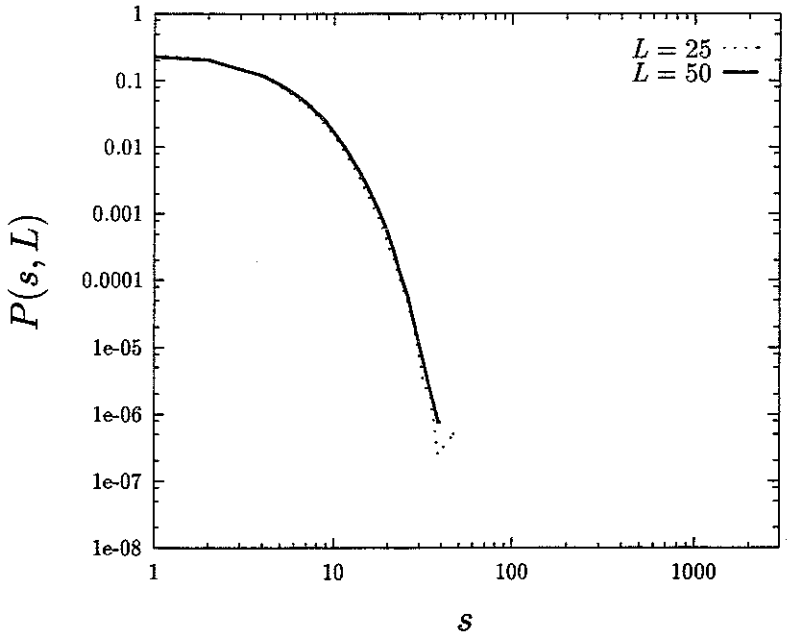

(a)

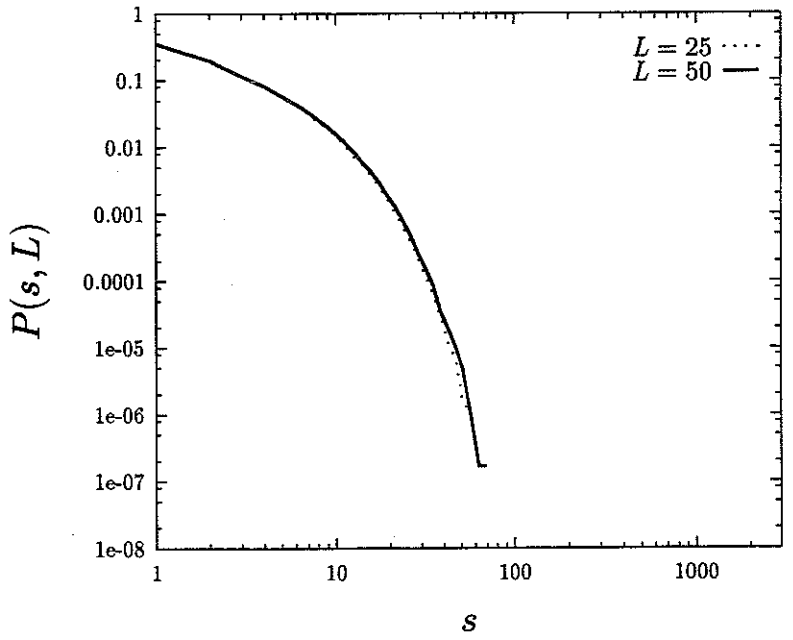

(b)

Fig. 4. The nonconservative stochastically driven Zhang model with $\varepsilon = 0.20$, $E_c = 1$, and $L = 25, 50$ when (a) $\delta E = 1$, (b) $\delta E = 0.2$, (c) $\delta E = 0.008$, and (d) $\delta E = 0.00032$.

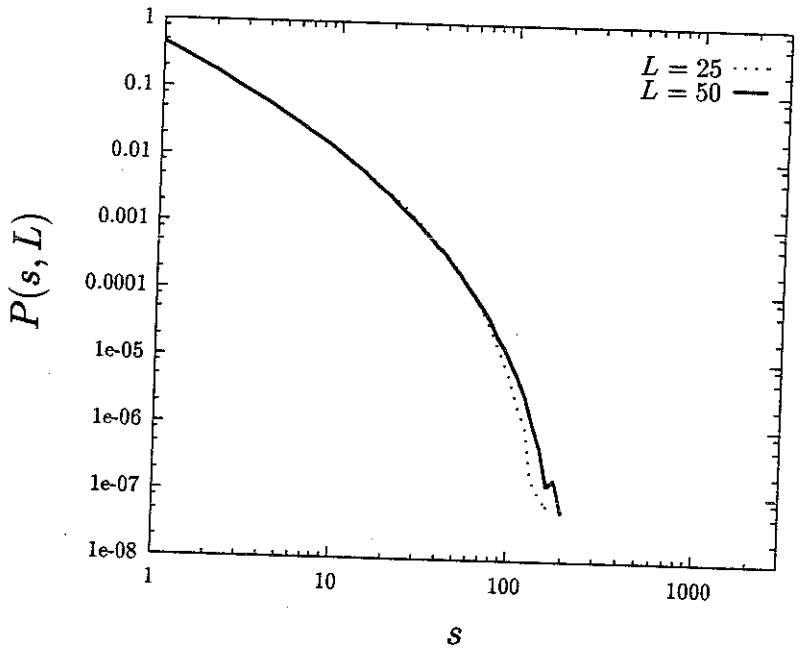

(c)

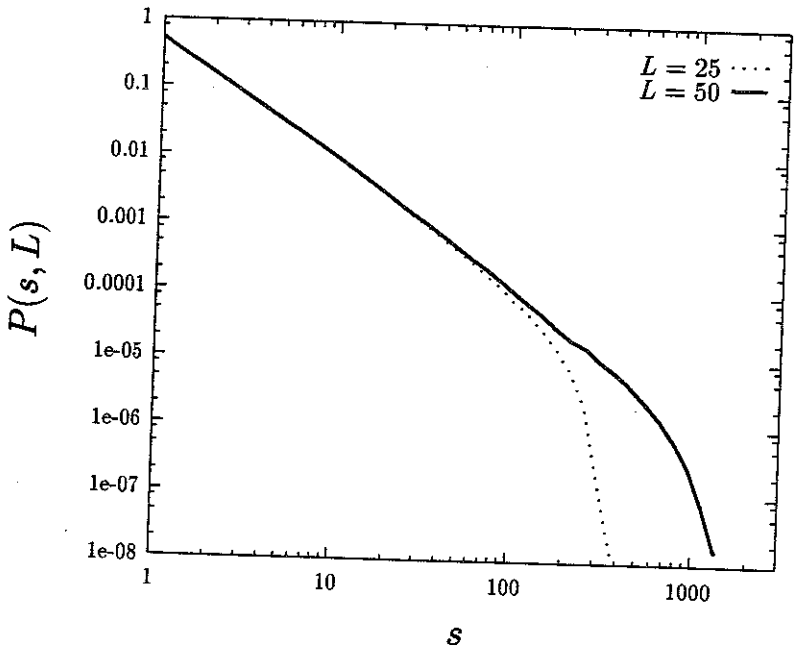

(d)

Fig. 4. (*Continued*)

3. Synchronization

Synchronization is a fascinating phenomenon observed in biological, chemical, and physical systems that has captivated the attention of many scientists in the last century. The paradigmatic example is observed in some forests of South Asia where, at night, myriads of fireflies are sitting in the trees. At the beginning, the members of the population emit flashes of light incoherently but after a short period of time the whole swarm is flashing in unison creating one of the most striking visual effects ever seen. But mutual coherence in the temporal activity of a group of units has been observed in other contexts. Some examples are the cell mitotic cycle, heart pacemaker cells, circadian pacemakers (biological clocks), neurons in the visual cortex, menstrual period of women, Josephson junctions, or some chemical reactions, just to cite a few. Winfree's book[53] is an excellent reference to read about these systems.

The relevance of synchronization has been stressed frequently although not always fully understood. In the case of fireflies it may help the courtship between male and female.[54,55] In the heart, the impulses coming through the vagus nerve trigger the contraction of the heart only if they are properly synchronized.[56] In other cases the relevance is still a matter of discussion. There are some evidences which support that coherent oscillations play an important role in sensory processing. It has been suggested that the discrimination and segmentation of objects, so often performed by living systems, can be explained by analyzing the temporal firing patterns of different neurons in the visual cortex.[57–60]

Which mechanisms are capable of generating a collective synchronous behavior? It is accepted that in order to observe a global coherent activity, oscillatory interacting units are required. The rhythmic activity of each element is provoked either by some internal processes or by external sources (external stimuli or forcing). The internal processes may have a physical or biochemical origin of great complexity, which probably is different for any of the systems considered above, but the essence of the phenomenon can be explained in terms of basic principles which allow us to create a common framework. Within this environment, a simple and general mathematical description can be formulated.

Suppose that the rhythmic activity of each element can be described in terms of a magnitude which evolves regularly in time. When such variable reaches a certain threshold value the unit emits a pulse (action potential for neurons) which is transmitted to all the members of the population connected to it. Moreover, a resetting mechanism initialize the state of the unit that has fired. Then, a new cycle recommences. Essentially the behavior is analog to an oscillator. Assuming that the period of the rhythm is T, it is convenient to define the concept of phase, without loss of generality defined in $[0, 1]$, which is a periodic measure of the elapsed time. In general, the phase is a nontrivial function of the state of the considered element. These features define the so-called relaxation or integrate-and-fire oscillators (IFO's).

Essentially, the effect of the emitted pulse is to alter the current state of the neighbors by modifying their periods. This change is not uniform; sometimes the period is lengthened and sometimes it is shortened. The perturbation depends on the current state of the oscillator which receives the external impulse. The modification induced by such a pulse can also be studied in terms of a phase-shift, what has been called phase response curve (PRC). Several different PRC's have been reported in the literature depending on the particular system under study.[61–63] In general, the analysis of the collective behavior of the system can be done in terms of a PRC if the phase-shift provoked by an impulse is independent of the number of impulses arriving within an interspike interval and if the arrival of such an impulse affects the period of the current interval but does not modify future intervals. This fact fostered a bunch of papers, published in the seventies and the beginning of the eighties, devoted to analyzing the different patterns of entrainment between pairs of pacemakers. However, a systematic treatment of the whole population was still missing.

There is another type of models where synchronization effects have been studied extensively. In these models each member of the population is modeled as a nonlinear oscillator moving in a globally attracting limit cycle of constant amplitude. These are the phase, or limit cycle, oscillators. The units interact weakly to ensure that any perturbation does not move any of them away from the limit cycle. Then, only one degree of freedom is necessary to describe the dynamic evolution of the model. Perhaps, the best known example is the Kuramoto model,[64] where the phase φ_i of each oscillator obeys the following Langevin equation

$$\dot{\varphi}_i = \omega_i + \sum_{j=1}^{N} J_{ij} \sin(\varphi_j - \varphi_i) + \eta_i(t)\,, \tag{16}$$

where ω_i is the intrinsic frequency of each member, and η_i denotes a Gaussian white noise of zero mean and correlation given by

$$\langle \eta_i(t)\eta_j(t')\rangle = 2D\delta_{ij}\delta(t-t')\,. \tag{17}$$

When there is no dispersion in the values of ω_i this model can be transformed into the planar XY model, well known in statistical mechanics. However, in the context of oscillators ω_i is picked from a random distribution. Note that the main difference between these phase-coupled oscillators and the pulse-coupled IFO's explained before is that now the coupling is not pulsating but it acts continuously in time, depending only on the phase difference between units.

For ferromagnetic all-to-all interactions ($J_{ij} = J/N, J > 0$), there is a critical value of the coupling strength J for which a phase transition occurs between a state where all the oscillators run incoherently with its own frequency to another state where a certain degree of synchronization appears spontaneously.[65,66] The nature of such transition depends on the distribution of frequencies,[67,68] on the features of the coupling,[69–72] and on the strength of the noise D.[73,74] In this review our interest

will be focussed on the pulse-coupled model although under certain conditions it is possible to convert a model of IFO's into a model of phase-coupled oscillators as has been shown by several authors.[75–77]

In general, three different levels of synchronization can be observed when considering populations. The strongest implies that all the oscillators have the same phase. When the members of a group do not fire in unison but keep a fixed phase difference between them, a "phase locking" regime is achieved. Finally, the weakest situation appears when several oscillators run with the same average frequency but without keeping any fixed phase difference. This is called "frequency locking".

A particularly interesting task was developed by Winfree who was one of the first authors who considered the population as a whole and who gave mathematical tools to tackle this problem.[78] His ideas were picked up by other scientists who developed them more deeply or proposed alternative mathematical techniques to solve problems which remained open for decades.[79] Mean-field models are sufficiently simple to be solved exactly and to analyze under which conditions any of the three levels of synchronization defined above can be observed.

3.1. *Mean-field models*

We will consider systems formed by an assembly of N identical IFO's with all-to-all couplings. Each member of the population is described in terms of a phase variable φ and a state variable E which evolve in time according to the following equations

$$\frac{d\varphi_i}{dt} = 1 \tag{18}$$

and

$$\frac{dE_i}{dt} = f(E_i) + g(E_i, t)\,, \tag{19}$$

where $f(E_i)$ is the driving rate, which gives the natural evolution of the oscillator, and $g(E_i, t)$ is a function that accounts for the effect of the coupling between unit i and the rest. It may have a complicated dependence on time. In this description self-interaction is not considered but we take an explicit dependence of $g(E_i, t)$ on the current state of the oscillator which receives the incoming input. The dynamics follows the essential trends mentioned in the introduction for relaxation oscillators. When an oscillator reaches the threshold it is reset ($E \to 0, \varphi \to 0$) and the rest of oscillators suffer a perturbation of their internal state. The features of this perturbation depend on $g(E_i, t)$. This description is quite general and includes the majority of models of integrate-and-fire oscillators studied so far. Moreover, it allows a straightforward generalization to models with nonidentical periods. We can see in this dynamics a first contact point with models which display SOC behavior. A particularly interesting case was considered by Mirollo and Strogatz (MS).[80] Their work was inspired in the analysis developed by Peskin[81] for the cardiac pacemaker, though the main outcomes are general enough to be applied to a wide range of models. MS consider systems whose intrinsic dynamics is given by a driving rate

$f(E)$ that satisfies

$$f(E) > 0 \quad \text{and} \quad f'(E) = \frac{df(E)}{dE} < 0, \quad \forall E, \tag{20}$$

that is, the state variable E and the phase φ are related through a convex function $E(\varphi)$, hereafter called the driving (see Fig. 5).

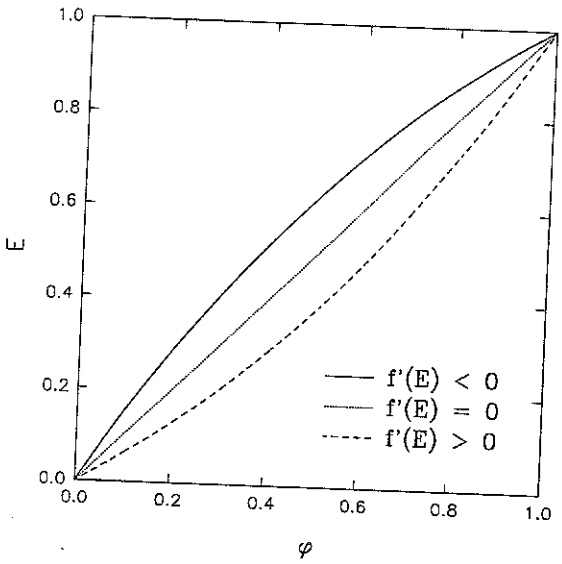

Fig. 5. Functional relation between the state of a unit E, and its phase φ, for different driving rates corresponding to a convex driving ($f'(E) < 0$), linear driving ($f'(E) = 0$), and concave driving ($f'(E) > 0$), respectively.

As an example, for the Peskin model[81]

$$f(E) = \gamma(C - E), \tag{21}$$

where γ is a constant that gives information about the convexity of the driving and $C = \frac{1}{1-e^{-\gamma}}$ ensures that the period is one when the threshold is one. This simplified model accounts for the variation of the membrane potential E (voltage difference between the internal and external part of a cell), as a consequence of the transport of Na, K and other ions across the membrane channels. The system is simply represented as an RC circuit, which implies $\gamma > 0$.[82,83]

On the other hand, in the MS model, the coupling between the oscillators is given by

$$g(E_i, t) = \varepsilon \sum_j \delta(t - t_j), \tag{22}$$

where the sum involves all the oscillators which have fired at a given moment (t_j denotes the time at which the jth oscillator fires). An equivalent description can

be made in terms of the state variable E

$$g(E_i, t) \propto \varepsilon \sum_j \delta(E_c - E_j)\,, \tag{23}$$

where now the sum runs over all the oscillators and E_c is the threshold. The coupling is instantaneous, excitatory ($\varepsilon > 0$), and constant since there is no dependence on E_i, which means that when a cluster of m members reaches the threshold simultaneously, the state of the other units is changed immediately according to

$$E \rightarrow E + m\varepsilon\,. \tag{24}$$

One of the effects of such pulse-like interaction is that when one oscillator fires other members can also reach the threshold. These oscillators may in turn push other elements up triggering an avalanche. In this case all the units which have fired merge in a group which does not break up anymore. This effect is called absorption. The concept of absorption implies the existence of a refractory time, a period where the oscillator which has fired is not sensitive to new incoming inputs. It has a crucial effect when the interaction is modeled in terms of a delta function, as we will see later. Notice that a coupling given by (22) implies the existence of two time scales, a slow scale for the intrinsic dynamics of the units and a fast one, indeed infinitely rapid when compared with the other, for the interaction between IFO's. Once again we can establish a connection with models displaying SOC. In terms of this time scale separation we can say that the refractory time only acts in the fast time scale.

MS were able to prove that for any $\varepsilon > 0$ the population of oscillators will be firing in synchrony in the stationary state for almost any initial condition (except in a set of Lebesgue measure zero) provided the driving is convex, i.e. when Eq. (20) holds. In fact, this result can be derived even with more restrictive conditions given by

$$g(E_i, t) = \varepsilon\delta(t - t_j)\,. \tag{25}$$

According to this description the strength of the pulse emitted by a group of oscillators is independent of its size, that is, there is no additivity in the coupling and therefore $m = 1$ in Eq. (24). This result is very powerful because (25) does not favor synchronization, just the opposite. When additivity is taken into account, the process of entrainment is accelerated and perfect synchrony can be found under broader conditions than those given by the MS theorem.[51,84]

Note that there is no contradiction in these results because the theorem only gives sufficient but not necessary conditions to synchronization (Eq. (20)). Figure 6 illustrates this situation.

The MS model has been generalized to other situations. It has been studied in the presence of weak noise[85] and with a random distribution of thresholds.[86] Some studies have emphasized the necessity to overcome some unrealistic features of the model. For instance, the instantaneous character of the coupling does not take into

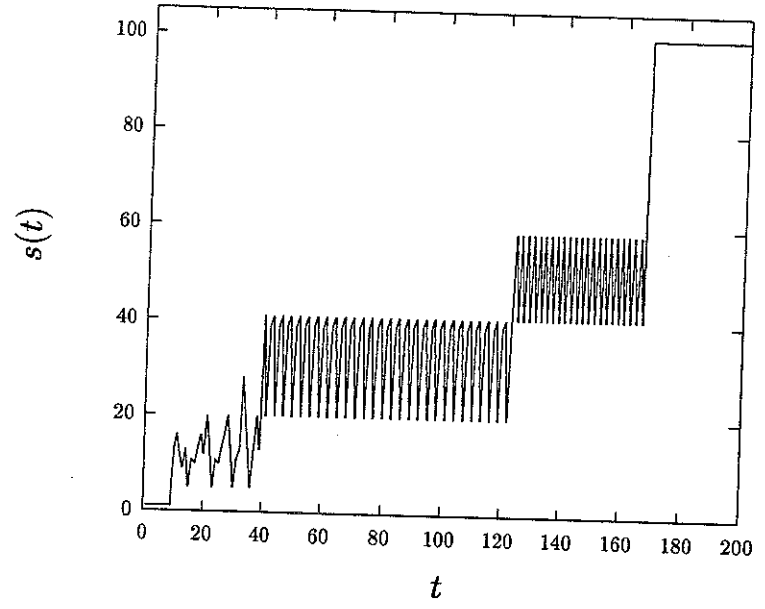

(a)

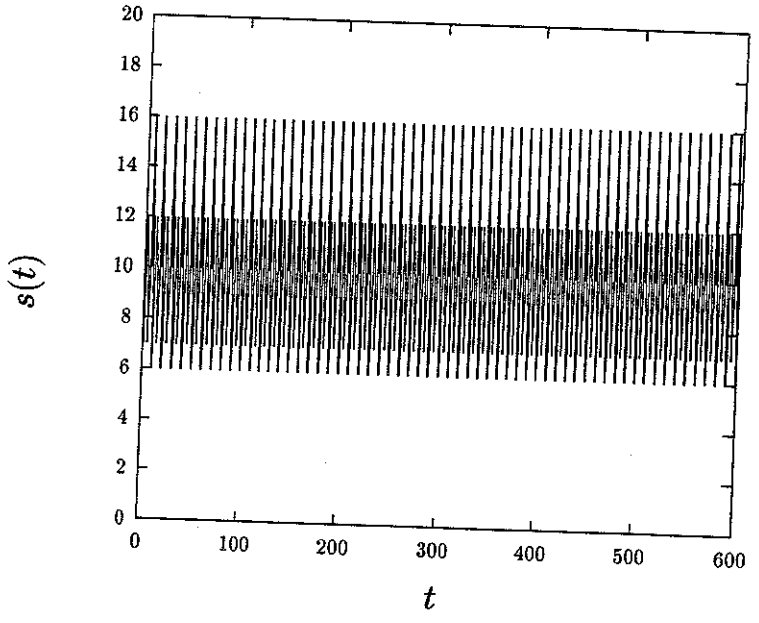

(b)

Fig. 6. Time evolution of the size of the "avalanches" for the Peskin model with all-to-all coupling, $\varepsilon = 0.1$, and $N = 100$. (a) A convex driving, $\gamma = 0.1$, leads to synchronization, and (b) with a concave driving, $\gamma = -0.1$, the system settles in a periodic state which is very sensitive to initial conditions. In these simulations we have considered the extreme situation given by Eq. (25). Time is measured in number of avalanches.

account the finite time of the synaptic response nor the finite time associated with the transmission of information propagating along the axons (delays). Both are relevant in models of spiking neurons and make the collective behavior much richer.[87–89] As an example, recent studies have shown that under certain conditions inhibitory couplings rather than excitatory lead to synchronization[90–92] in agreement with some experimental observations.[93] These results contrast with the MS model for inhibitory coupling ($\varepsilon < 0$). A straightforward revision of their proof shows that the sufficient conditions to find synchronization in this case are $f(E) > 0$ but $f'(E) > 0$, $\forall E$.

Another underlying hypothesis that restricts the range of interest of the MS model concerns the strength of the coupling ε which does not depend on the state of the oscillator which receives the pulse. As we have mentioned above, in many studies of biological pacemakers it is assumed that the response of a cell due to an external stimulus is a phase shift (given by the PRC) which induces an energy-shift $\varepsilon(E)$ in Eqs. (22) or (25), hereafter called the energy response curve (ERC), that, in general, is a nonconstant function of E. It is possible to generalize the MS theorem by considering a general ERC as well as an arbitrary driving rate, with the only restriction of having $f(E) > 0$. Then, a sufficient condition to find a stable synchronous regime is given by[94]

$$\frac{f'(E)\varepsilon(E)}{f(E)} < \varepsilon'(E), \quad \forall E. \tag{26}$$

This means that, in general, the knowledge of the intrinsic dynamics (i.e. the driving) of an individual oscillator is not enough to predict the final state of the population. Information about the response of a given unit in the presence of an external stimulus is also required.

3.2. *Short range models*

The question of whether the conclusions extracted from the MS theorem can also be applied to lattice models with short-range connectivity is of great importance. First, notice that in mean-field models synchronization emerges in an absorption process, where clusters of oscillators of increasing size merge with each other and never break up. However, in a lattice model, big assemblies of oscillators with the same phase, which eventually may break up, are generated by means of avalanches that start at a given point and propagate through the lattice. When they sweep the whole system we call them relaxation oscillations. Therefore, due to the different nature of both mechanisms one would expect that the conditions required to find synchronization/relaxation oscillations are different. In general, it is not easy to get analytical results for short-range models. Only for very special bc and for systems of low dimensionality (essentially $1D$) exact results have been derived.[95] Therefore, in the majority of situations the main outcomes rely on computer simulations. As we will see later, they show that under certain conditions mean-field arguments can be extrapolated to systems with finite connectivity.

Let us consider a lattice model of IFO's with local rules given by (19) and (22) (but now the sum runs only over nearest neighbors). An important point concerns the way in which an avalanche is propagated through the lattice. Suppose that a given unit, the seed, has fired and as a consequence some of its neighbors reach the threshold. In turn, these oscillators will fire, interacting with their neighbors being the seed among them. The question is what happens with the seed. According to the strategy applied in the mean-field version of the MS model such unit should remain at the reset point during the whole avalanche. This is important because such effect implies the existence of a refractory time which persists until all the oscillators are below the threshold. Furthermore, all the members which have fired will have zero phase when the avalanche is over. We can describe this refractory time by an ERC that verifies $\varepsilon(0) = 0$. Under such conditions computer simulations show that relaxation oscillations appear when $f'(E) < 0$ and ε is a definite positive constant, in agreement with a conjecture proposed by MS.[80] For a more general function $\varepsilon(E)$ (but $\varepsilon(0) = 0$), it has been shown[94] that (26) is a sufficient condition to observe relaxation oscillations. Moreover, in this case relaxation oscillations lead to a perfect synchronous regime.[c] Figure 7 gives numerical evidence of this fact.

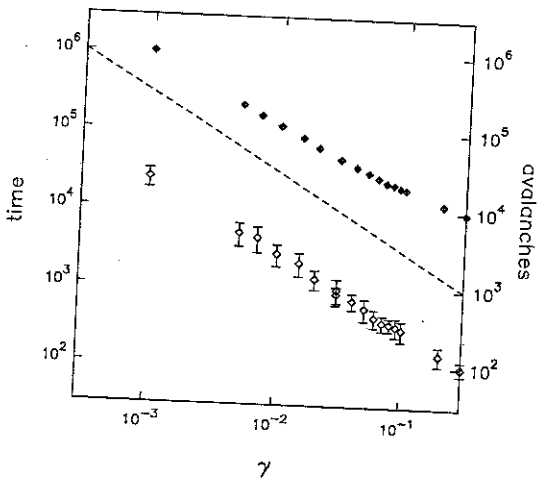

Fig. 7. Number of avalanches (filled) and time in period units (hollow) required for a 32×32 lattice of Peskin's oscillators with open bc to observe complete synchronization as a function of γ in a log – log scale. The straight line shows the γ^{-1} behavior. The value of ε is constant and equal to 0.1. Similar results are obtained for periodic bc and other driving rates.

The most appealing consequence of the previous results is that for coupled dynamical systems like those considered before, for open or periodic bc, mean-field

[c]Note that for open bc and $\varepsilon(0) \neq 0$, after a relaxation oscillation of the size of the system not all the units have the same phase. For instance, the cells located at the boundaries remain at a different state with respect to those located in the bulk because the number of neighbors in each case is different.

results seem to be still valid and represent sufficient conditions to ensure the existence of the synchronized regime, provided one considers the refractory time.

When the driving is linear, the phase and the energy become identical. In this case, for a constant ERC, it is very simple to show that starting from a random initial configuration the system evolves towards a periodic state formed by clusters of oscillators with the same phase. The phase difference, after a cycle, remains constant in time once all the units have fired, and consequently the system does not synchronize in agreement with Fig. 7. On the other hand, a concave driving may give rise to the appearance of stable complex phase-locked spatio-temporal structures[94,96,97] as, for instance, a chessboard-like configuration. This sort of "antisynchronized" states are exclusive of the short-range models since there is no counterpart in the mean-field case.

On the other hand, we could suppose in the previous discussion that the seed was updated as any other neighboring cell, that is, $\varepsilon(0) \neq 0$, so the refractory time is removed. In that case the coupling between neighbors is governed, when $E_{ij} \geq E_c$, by

$$\begin{aligned} E_{nn} &\to E_{nn} + \varepsilon\,, \\ E_{i,j} &\to 0\,. \end{aligned} \tag{27}$$

These rules are not new. They were introduced in a stick-slip model by Feder and Feder (FF)[98] in the context of earthquake dynamics, with the restriction of having a constant driving rate and open bc.

As in all the models of IFO's discussed so far, since the relaxing site is reset to zero and a fixed amount is transferred to the neighbors, the FF model does not have any memory of the initial configuration. After an avalanche, all the sites that have fired have an energy which is a multiple of ε. When the threshold E_c and ε are commensurable, that is E_c/ε is an integer M, the system eventually reaches a state with M distinct values of the dynamical variables. Hence, after an avalanche, $E_{i,j} = n\varepsilon, n = 0, \ldots, M-1$, and since the driving is uniform, $E_{i,j} = n\varepsilon, n = 1, \ldots, M$ when initiating an avalanche. When E_c is incommensurable with ε, that is, when E_c/ε is not an integer, the system is not able to reach a "partially synchronized" state. Figure 8(a) displays the average number of totally synchronized sites as a function of time for $E_c/\varepsilon = 4, 100/22$, and 5. When E_c is commensurable with ε, the time the system needs to settle down into such a state increases as ε decreases. Note that the case of $M = 4$, was originally studied by Feder and Feder.[98] Their results are quite different. This will be explained in detail in the next section. Figure 8(b) displays the corresponding distributions of avalanche sizes. When $M = 4$ and 5 only large avalanches are seen. For $M = 100/22$, avalanches of all sizes occur, but they are not power-law distributed.

4. Synchronization and Self-Organized Criticality

Up to now, we have seen the strong similarities between some models displaying SOC and lattice models of IFO's showing different levels of synchronization. In

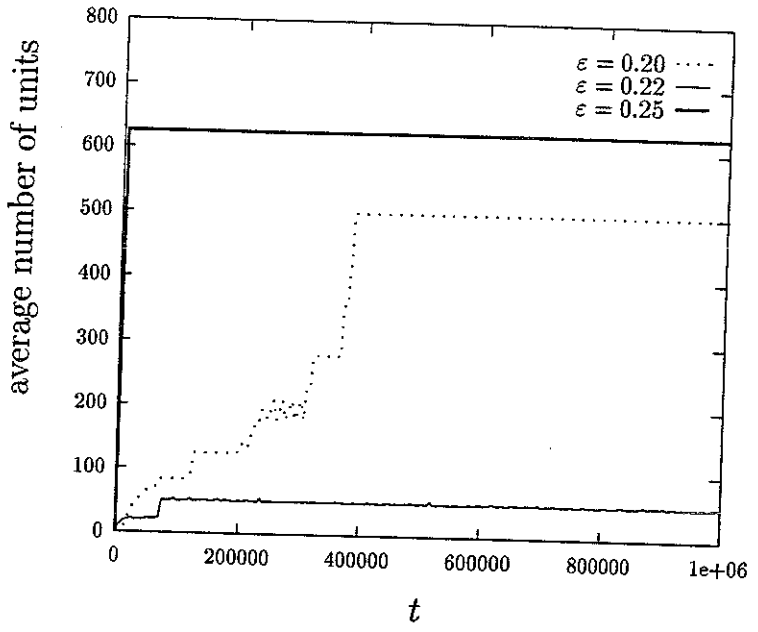

(a)

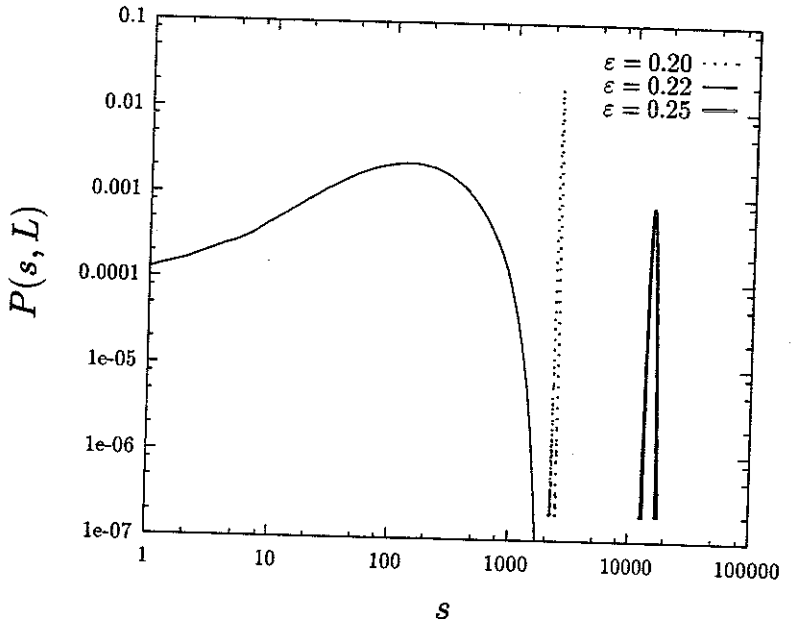

(b)

Fig. 8. (a) The average number of synchronized sites in the FF model with $\varepsilon = 0.20, 0.22$, and 0.25, respectively. $E_c = 1$ and system size $L = 50$. (b) The corresponding avalanche distribution when the system has reached the final partially-synchronized state. Time is measured in number of avalanches.

both types of systems, each unit has an intrinsic dynamics leading to a threshold value. When this threshold is reached, the unit interacts with its neighbors and it is reset. This process is developed in a time scale much faster than that associated with the natural driving of each unit. The features of the couplings, the natural dynamics, and the reset mechanism define each particular situation. In view of this analogy it is reasonable to think that a general framework may be developed. We have shown that by an appropriate choice of the relevant parameters of these models a wide spectrum of collective behaviors can be observed. However, up to now our attention has been focussed on systems which display either SOC or any sort of phase locking. The goal of this final section is to move a step forward by showing that there is an interesting group of models, with quite different origins, which display both behaviors.

4.1. *Integrate-and-fire oscillators*

Let us start the discussion with a model studied in the previous section. We have seen that the FF model tends to develop, in the stationary state, either assemblies of cells with the same phase (when the ratio E_c/ε is an integer) in which case the big avalanches take place because a lot of units reach the threshold simultaneously or a more complex behavior (when E_c/ε is not an integer) where avalanches of all sizes take place, but they are not power-law distributed. These behaviors are not robust to noise.[51] In principle, the effect of the noise is to prevent two sites from becoming critical simultaneously due to the uniform driving. The nature of such noise can be based on the existence of fluctuations: on the dynamic variables, on the thresholds, or on the reset energy.[51,99] This source of dynamical noise has to be distinguished from a quenched source of noise, as for instance, a random distribution of frequencies.[100]

The dramatic effect of noise on the features of the stationary state of the model is observed in Fig. 9. When altering the relaxation rule (27) slightly by adding a small random number in the range $[0, 0.001]$ to the reset oscillator,[51] the system no longer settles into a state with a few groups of oscillators with the same phase, but it goes towards a new state in which the avalanche distribution follows a power-law decay characteristic of SOC.

Keeping in mind the results given in the previous section for the MS model, it is not difficult to imagine that by increasing the convexity of the driving (in the original FF model it is linear) SOC fades out, even in the presence of a dynamical noise,[d] and for a certain degree of convexity a spatial structure formed by large groups of oscillators with the same phase appears spontaneously.[101] In fact, the features of the model allow us to derive analytically an explicit condition, written

[d]Corral *et al.*[101] introduced the noise by choosing at random one of the cells that become critical simultaneously due to the driving and making it the starting point of the avalanche, while the energy of the rest of critical cells was decreased by a small random amount. However, different sources of dynamical noise give similar results.

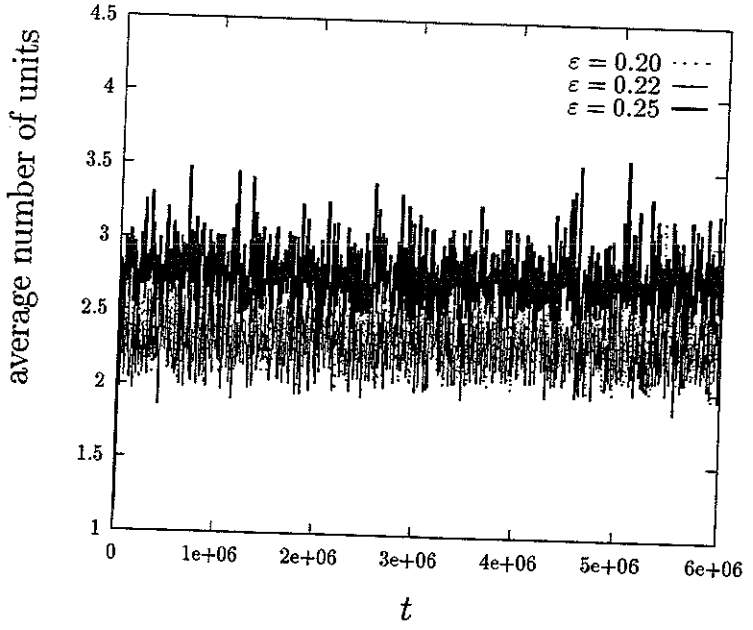

(a)

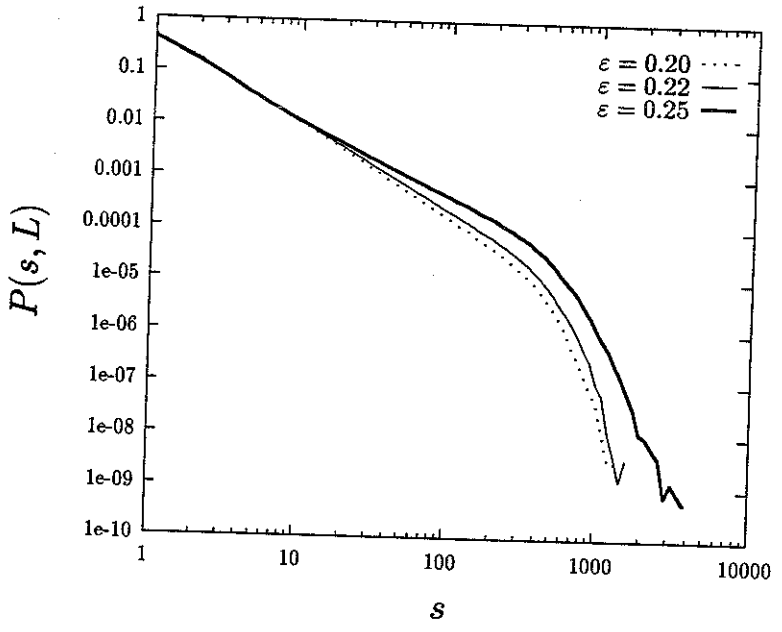

(b)

Fig. 9. The FF model ($L = 50$ and $E_c = 1$) with dynamical noise. (a) The average number of totally synchronized oscillators. As in previous figures time is measured in terms of the number of avalanches. (b) The distribution of avalanche sizes are power laws where the slopes change with ε.

in terms of a critical convexity γ_c, which ensures that a state characterized by the existence of relaxation oscillations of the size of the system is a fixed point. However, this argument cannot ensure that such fixed point is an attractor. We will show, by numerical simulations, that it has a large basin of attraction.

Let us assume that there is an avalanche sweeping the whole lattice (for an arbitrary geometry). The idea is to derive a condition that could ensure that the next event will reach the whole population as well. Let n denote the lattice coordination number and m the number of neighbors of the most unfavorable site (the cell or group of cells with the smallest number of neighbors). These sites have zero energy when the avalanche is over, and in order to fire in the next avalanche, they have to satisfy[101] (for excitatory coupling),

$$E\left(1-\varphi(n\varepsilon)\right)+m\varepsilon \geq E_c\,. \tag{28}$$

In the case of the Peskin model the relations between the phase and the energy are

$$E(\varphi)=C\left(1-e^{-\gamma\varphi}\right) \tag{29}$$

and

$$\varphi(E)=\frac{1}{\gamma}\ln\frac{C}{C-E}\,, \tag{30}$$

where C was already defined in (21). A simple calculation yields, when $E_c=1$,

$$\varepsilon \leq \frac{C(m-n)+n}{mn} \tag{31}$$

which is the relation between ε and γ that must be satisfied for model (21) with interaction rules (27) in order to show relaxation oscillations involving all the cells. In the particular case of a regular $2D$ square lattice with open bc, the most unfavorable sites are the corners. Hence

$$\varepsilon \leq \frac{2-C}{4}\,. \tag{32}$$

This relation has been checked through simulations finding an excellent agreement as can be seen in Fig. 10. In region A, the condition (32) is satisfied and therefore, the system settles in a state where a macroscopic group of oscillators whose size scales with the size of the lattice remain at the same phase. In region B, the condition is not satisfied and relaxation oscillations involving all the cells are not stable. The system goes towards an attractor of difficult classification whose characteristics will be discussed later. In the limit of $\gamma=0$ we recover the features of the noisy FF model. Notice that a convex driving is not enough to find relaxation oscillations. It is necessary to go beyond γ_c. In fact, γ_c tends to $\ln 2$ in the limit of $\varepsilon \to 0$.

When considering periodic bc in a $2D$ square lattice, Eq. (31) reads

$$\varepsilon < 0.25 \tag{33}$$

thus favoring the appearance of relaxation oscillations in the sense discussed above: it is a stable fixed point but, in principle, we cannot ensure it is an attractor for

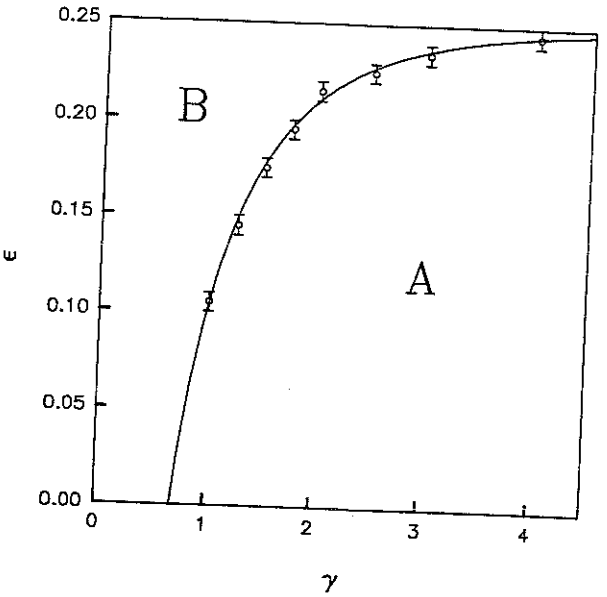

Fig. 10. Schematic phase diagram in terms of γ (the convexity of the driving) and ε (the strength of the coupling) for model (27) and units driven by (21). The symbols correspond to the phase transition observed in the simulations and the error bars are given by the standard deviation over ten measures. The solid line corresponds to the analytical result (32).

the dynamics of the system. Indeed, numerical simulations show that this synchronized state can be an attractor of the dynamics in some cases. This model has also been analyzed by Hopfield and Herz[102,103] in the context of computation by networks of integrate-and-fire neurons. These authors study a general model with interaction rules[102]

$$\begin{aligned} E_{nn} &\to E_{nn} + \varepsilon\,, \\ E_{i,j} &\to \Gamma(E_{i,j} - 1)\,, \end{aligned} \tag{34}$$

and a linear driving. This model is equivalent to the FF model in the $\Gamma = 0$ limit and to the uniformly driven BTW when $\Gamma = 1$. As soon as every element has fired once, the system reaches a limit cycle in which each oscillator fires exactly once during one period of the oscillation, no matter the value of Γ. For the BTW model it is possible to construct a Lyapunov function that shows this convergence. However, for $\Gamma < 1$, the volume of the attractor is greatly reduced. From numerical simulations on $2D$ square lattices they construct a diagram in terms of the initial distribution of energies and the coupling strength ε. The behavior ranges from a trivial fully synchronized state, when the initial distribution of the oscillators is very narrow, to an exponential distribution of events, when the initial distribution is broad enough. In the border line between both regions a power-law distribution of events is reported. The same authors[103] have also studied the limiting cases of the BTW and FF models with units being driven nonlinearly. Within the computational

aspects of this work they perform simulations from which one can conclude that all the models exhibit rapid convergence to periodic solutions with locally synchronized clusters. However, in the large time scale the behavior is quite different. In this case, the BTW interaction rules lead to a global synchronization whereas FF's show a partially synchronized behavior. The existence of this nonglobal synchronized periodic state for the FF model confirms that Eq. (33) gives the existence of a synchronized state (in the sense of a simultaneous firing of all the units) that, however, it is not necessarily a global attractor for the dynamics. These authors give conditions which show that if the strength of the coupling is strong enough, a simple spatially nonuniform periodic solution is also possible.

4.2. *Spring-block models*

Now, we are going to analyze the effect of a nonlinear convex driving in deterministic spring-block models, such as those discussed in the context of earthquake dynamics, which display SOC with a linear driving.[10,47,104] As in models of IFO's, these nonlinearities tend to break SOC in favor of more complex dynamical states. However, there are several differences that must be remarked. In the OFC model (7) two cells very seldom reach the threshold simultaneously and trigger an avalanche in two different points of the lattice. There is no need to introduce a dynamical noise in contrast with the FF model where the existence of the noise is required to observe SOC. Therefore, concerning the SOC behavior, one might conclude that the existence of some kind of noise, either in the way the system is driven or in the initial conditions, is necessary. On the other hand, some authors have reported power-law distributions for completely deterministic automata.[105,106,107] However, for all these deterministic models there is a single site with a special behavior; this inhomogeneity, either in the initial conditions or in the external loading, is what gives rise in these cases to the complex behavior characteristic of SOC.

For the OFC model it is also possible to deduce analytical results giving information about the conditions required to observe a transition between a regime where relaxation oscillations rule the long time behavior and other dynamical states. However, the situation here is more difficult and two equations are necessary. One ensures that the avalanches will reach all the cells of the lattice, and the other is based on the assumption that the configuration after a big event always will be the same. The main difference with respect to the FF model is that we have to replace ε by an effective value $\bar{\varepsilon}$ since the energy of a given site can be larger than $E_c = 1$ when the avalanche propagates through the lattice.[e] Within a mean-field approximation we will assume that this energy is the same for all cells, except the seed (the unit that triggers the avalanche), its neighbors and the boundaries. Assuming that any site fires at most once during an avalanche[f] the seed has a phase $\varphi(4\bar{\varepsilon})$ when the

[e]Actually, for a regular $2D$ square lattice $\bar{\varepsilon}$ is bounded between ε and 2ε since the energy at any site cannot exceed the value of 2.

[f]This can only be ensured when $\varepsilon < 0.22$.[49]

avalanche has finished, and to fire again it has to increase by an amount $1-\varphi(4\bar{\varepsilon})$. Since its neighbors are at $\varphi(3\bar{\varepsilon})$ the condition to repeat permanently this situation is

$$4\bar{\varepsilon} = 4\varepsilon \left[E\left(\varphi(3\bar{\varepsilon}) + 1 - \varphi(4\bar{\varepsilon})\right) + \varepsilon\right] . \tag{35}$$

This equality, in addition to (31), with ε replaced by $\bar{\varepsilon}$, gives the following relationship between ε and γ

$$\varepsilon \leq \frac{1}{16}\left[\sqrt{C^2 - 52C + 164} - (C+6)\right] . \tag{36}$$

When this condition is fulfilled, only relaxation oscillations of the size of the system can survive in the stationary state. The curve corresponding to the equality has been plotted in Fig. 11 (solid line). It has been corroborated through simulations performed in a system of size 64×64 with a fixed value of γ and increasing ε from below. For 10 different realizations of the initial random conditions we look at the final state after $3 \cdot 10^6$ avalanches. The average value of ε where the transition is observed corresponds to the circles in Fig. 11 and the error bars correspond to the standard deviation.

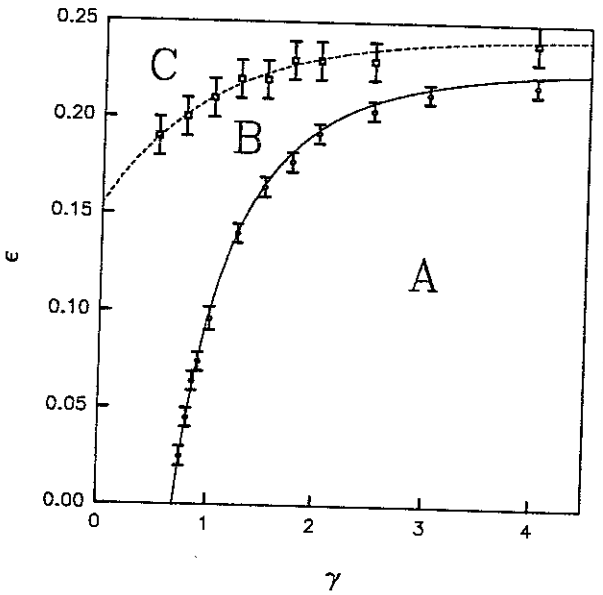

Fig. 11. Schematic phase diagram in terms of γ (the convexity of the driving) and ε (the strength of the coupling) for the OFC interaction rules with a driving given by (21). The symbols correspond to the phase transitions observed in the simulations. For the B-C transition the error bars denote that above them we have always found SOC while below them there is no power-law behavior. For the A-B transition the error bars are given by the standard deviation over ten measures. The solid line corresponds to the analytical result (36) and the dashed line is an exponential fit to the numerical data.

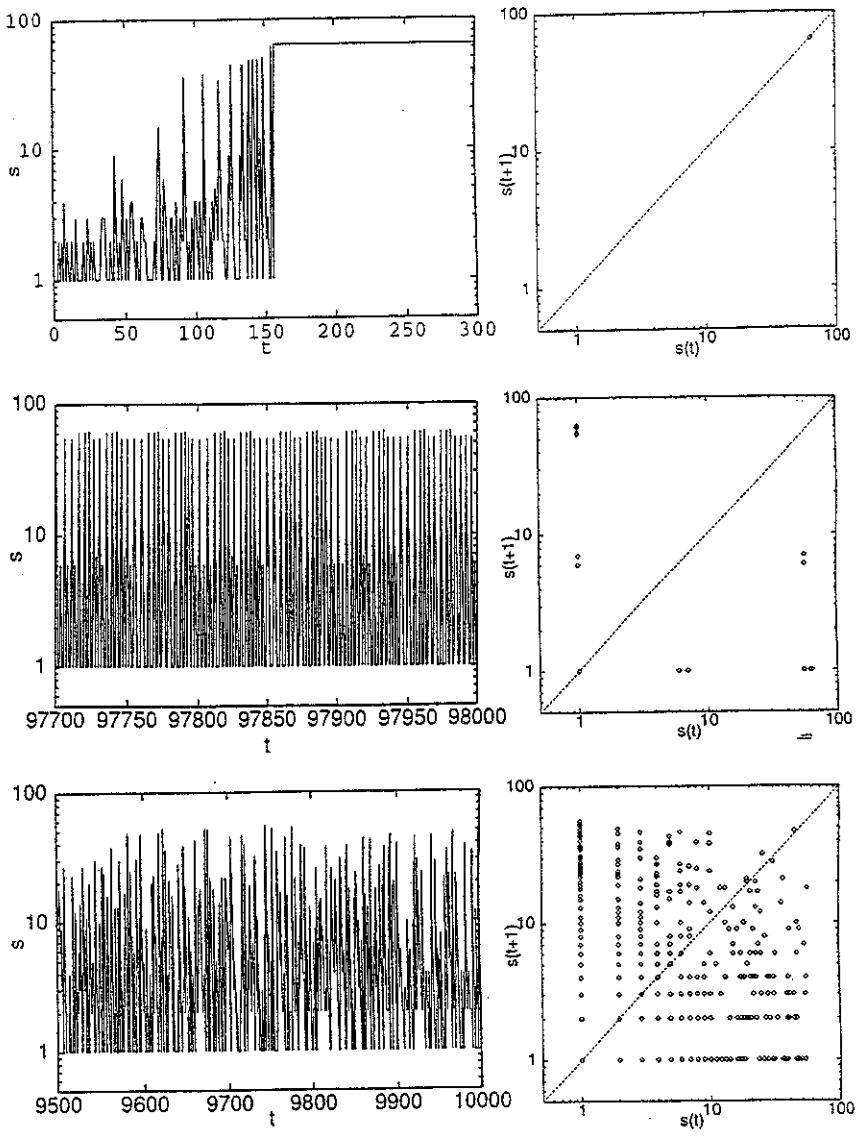

Fig. 12. Left column: Time evolution of the avalanche size. Right column: return map of the avalanche size. Top: in region A of Fig. 11 for $L = 8$, middle: for region B (close to region A), and bottom: for region C. Each time step corresponds to an avalanche.

Furthermore, to complement and illustrate the features of the dynamical states observed in the phase diagram of the model, we have plotted in Fig. 12 the time evolution of the avalanche size as well as its return map, for a particular run. Thus, we can clearly see that, in region A (Fig. 12(a)) large avalanches appear frequently until an avalanche sweeps the whole system and this state is maintained. On the other hand, the return map shows the evolution of the system at the fixed point. Let

us remind that in the theoretical approach we made the assumption that a whole system avalanche does exist. In the simulations one observes that this hypothesis is indeed true. The synchronization of the cells is not global but the number of cells with the same phase is of the order of the size of the system.

Slightly above the curve given by Eq. (36) an avalanche sweeping all the lattice cannot repeat any more since the next one will be unable to reach some of the cells in the boundaries and these cells will be the starting point of future avalanches (region B). This fact gives rise to a periodic behavior with a discrete distribution of a few avalanche sizes that can eventually be broken only by the effect of the dynamical noise. This is indeed what we have observed in the simulations; only some values of avalanche sizes are present. The exact location is very sensitive to the initial random configuration but they are always of order 1, L, and L^2. In Fig. 12(b) we show the time evolution of the avalanche size in a typical run in this region after a transient time. Here we can notice the appearance of the periodic state and a small number of points in the return map.

By increasing ε we observe that the distribution of avalanche sizes, $P(s)$, becomes continuous in the sense that all bins of exponentially increasing width have at least one event, up to some system size dependent cutoff. The transition from a sparse distribution to a "continuous" one would require a careful investigation. When $P(s)$ has this continuous appearance there are peaks at some characteristic lengths, roughly at L, $2L$, $3L$, ..., as can be seen in Fig. 13, and no finite-size scaling is possible.

By increasing ε again we observe that the intensity of the peaks decreases. Up to the system sizes and number of avalanches we have studied, there exists a transition to a stationary state with a power law, followed by an exponential decay of $P(s)$. We have identified the transition from regions B to C (squares in Fig. 11) by fixing γ and increasing ε up to the appearance of a finite-size scaling in the distribution of avalanche sizes. The dashed line is an exponential fit of the numerical results that we extrapolate to the linear driving case ($\gamma = 0$) and for large values of the convexity of the driving.

The criticality of the SOC state stems from the lack of characteristic time and length scales and for the apparent unpredictability of the size of the next event. This can be visualized in Fig. 12(c) where no simple correlation can be extracted from the time sequence. Just at the conservation line, $\varepsilon = 0.25$, where the interaction between units is stronger, we find SOC for a wide range of values of γ with a power-law decay over more than three orders of magnitude and the corresponding finite-size scaling as shown in Fig. 14.

Up to now we have studied a population of identical oscillators, with intrinsic period $T = 1$, but in a real system it is usual to find it randomly distributed. We have consider a uniform distribution, centered at $T = 1$.[100] For model (9) and a convex driving the results remain qualitatively the same for a width in the distribution as large as $0.1T$. However, if the width is equal to the mean period T the region where synchronization is observed almost disappears as well as SOC

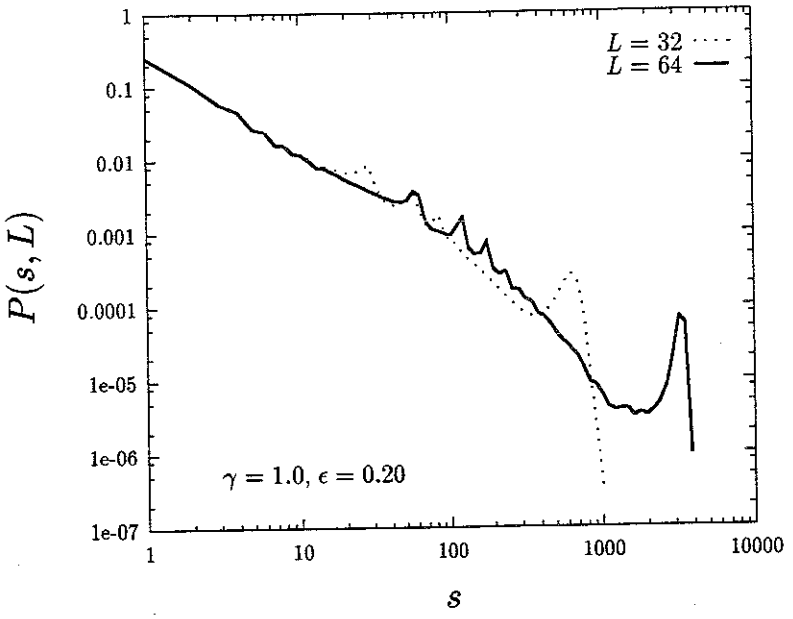

Fig. 13. Distribution of avalanche sizes in region B (close to region C).

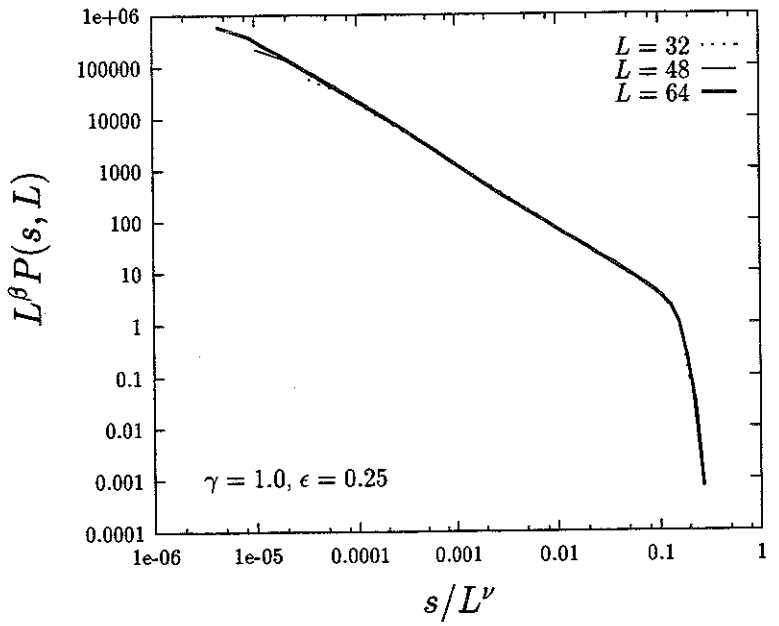

Fig. 14. Finite-size scaling ansatz of the distribution of avalanche sizes in region C. In this case $\tau = 2.2 \pm 0.1$, $\beta = 3.7 \pm 0.1$, and $\nu = 3.0 \pm 0.1$.

which is constrained to a narrow region near the line $\varepsilon = 0.25$. The effect of a quenched distribution of thresholds has also been analyzed by Janosi and Kertész (uniform distribution)[108] and by Torvund and Frøyland (Gaussian distribution)[109] for the linearly driven OFC model, where it has been shown that the distribution of avalanche sizes has an exponential decay for a sufficiently large spread.

A slightly different model with a uniform driving was analyzed by Socolar, Grinstein, and Jayaprakash.[104] In this case when a site reaches a critical value the interaction rules are

$$\begin{aligned} E_{nn} &\to \Lambda E_{nn} + \varepsilon E_{i,j}\,, \\ E_{i,j} &\to 0\,. \end{aligned} \tag{37}$$

In this model, $\Lambda \neq 1$ is a simple way to remove degeneracy, though it does not model the elastic nonlinearities of the blocks and springs model in detail. Rules (37) can be seen as a kind of a state dependent transfer (ERC), which can be transformed into a uniform transfer model with a nonlinear driving by means of the appropriate transformation.[90,94] When open bc are considered, $\Lambda = 1$ corresponds to the original OFC model and in an interval around this value there are indications of SOC behavior. Nevertheless, for $\Lambda < 1$, the authors suggest the observed behavior might correspond to a periodic state with either a long transient or a long period. For $\Lambda \geq 1$, the power law decay in the avalanche size distribution observed is related to apparently chaotic oscillations in the average energy

$$\langle E \rangle = \frac{1}{L^2} \sum_{i,j} E_{i,j}\,. \tag{38}$$

It is suggested that the boundary sites, which have a different cycle than interior sites, might be the source of the criticality observed. This issue has been analyzed in detail by Middleton and Tang[99] in a simple directed model; they show that the slower growth rate of the boundary sites favors the creation of synchronized clusters of all sizes. At a fixed time, the number of clusters of size d has a power-law tail that is independent of ε, $n(d) \approx d^{-\sigma}$. An avalanche can then eventually cross a cluster boundary whenever both clusters have close enough values of the energy, and this makes the avalanche size distribution to be also a power law.

As we noticed for the FF model, also for the OFC model a very important role is played by the bc. In particular, periodic bc break completely the SOC behavior and can provide some hints on its origin in the nonconservative continuously driven models.[99,104,50] For instance, Socolar, Grinstein, and Jayaprakash obtain[104] different behaviors, depending on the values of Λ in (37). Thus, for $\Lambda < 1$, the system always settles in a periodic state, with transients that become longer as Λ approaches one. On the other hand, for $\Lambda > 1$ the most common states are periodic with a cycle consisting of single avalanches that sweep the whole lattice. A simple picture can be obtained by analyzing the return map of a two-site model: for $\Lambda > 1$ both sites fire in the same avalanche, whereas for $\Lambda < 1$ there is a stable fixed point. These results are in agreement with the ones obtained for a nonlinear

driving by means of the above-mentioned transformation.[94] Finally, the special case of $\Lambda = 1$, shows a completely different behavior from what is expected from the limits of the previous cases: the system rapidly settles into a periodic state with avalanches of size one which are marginally stable as those described previously for the FF model.[102,103] Grassberger,[50] by means of very large-scale simulations, realized that there exists a close relation between temporal and spatial ordering; while time ordering is associated with the periodic behavior and becomes stronger as ε decreases, spatial order is related to the synchronization of neighboring sites which, in principle, seems to be favored by a large interaction between units. Concerning the SOC behavior, one can conclude that open boundaries create an inhomogeneity which prevents time ordering but spatial local ordering is still maintained. Along this line Middleton and Tang[99] have observed that by including some source of dynamical noise the system with periodic bc is periodic in time, after a brief transient time, and that these states are neutrally stable.

A different way to introduce the inhomogeneity that is responsible for the SOC behavior has been followed by Torvund and Frøyland.[109] They have considered a single site to have a threshold larger than the threshold of the remaining sites, in a system with periodic boundary conditions. These authors have found some evidence for a SOC behavior when the larger threshold is above a critical value. Nevertheless, also a non-simple periodic behavior can be observed. This means that a more careful analysis would have to be performed along this line.

4.3. *Other models*

Forest-fire models are other systems where typical SOC behavior has been observed.[11] The model is defined in a D-dimensional lattice (usually $D = 2$). Each site of the lattice is either occupied by a tree or empty. Trees grow according to a certain function that depends on the age of the empty site. A tree burns if it is struck by lightning with a small probability f. In this case, the fire propagates through the neighbors burning the whole cluster that immediately becomes empty.

In this system the features of the stationary state depend strongly on the specific form of the tree growth. Drossel[110] has shown analytically (for a $1D$ system) and through simulations that if the life-time distribution of empty sites has a long-time tail a SOC state with non-universal exponents is observed. On the other hand, for deterministic tree growth a coherent temporal activity between trees in the same cluster comes up. Therefore, we see again the relevance of the driving in the collective properties of the model.

Inspired by a forest-fire model, Clar, Drossel, and Schwabl[111] have studied a nonequilibrium percolation system which displays several behaviors ranging from SOC to clusterization. The authors consider a population of objects (trees, animals or others) distributed randomly over a lattice. The density of occupied sites is ρ. Then, a given site is chosen. If it is not empty an "explosion" occurs affecting all the neighbors within the same cluster, whose spatial position on the lattice is

redistributed (a group of animals dispersed by the action of a predator could be another example). In these terms the density of the system is a conserved quantity.

In the stationary state the model shows different regimes depending on the density of occupied sites of the lattice. For diluted networks ($\rho < \rho_1 = 0.41$) only small clusters of units are developed. As a consequence, the average number of units affected by an explosion and the size of the largest cluster $s_{\max}$ is small. For $\rho_1 < \rho < \rho_2 = 0.435$ the size of the explosions diverge but more slowly than the size of the system. They show that the relevant quantities diverge as a power law, with an exponent that depends on the density ρ. This critical behavior is characteristic of SOC. Finally, for larger values of the density there is a region where the explosions have infinite size (they scale with the size of the system) which is repeated periodically in time.

Related to this model we can notice the work of Csilling *et al.*[112] about dynamics of populations. Each site on a lattice denotes a population that evolves according to

$$N_{i,j}(t+1) = \lambda N_{i,j}(t)\,[1 + aN_{i,j}(t)]^{-\beta} \tag{39}$$

until a critical population density is reached (overcrowding). In this case a dispersal movement (migration) is triggered through nearest neighbor local habitats

$$\begin{aligned} N_{nn} &\to N_{nn} + \Delta\tfrac{N_{i,j}-N_{sc}}{4}\,, \\ N_{i,j} &\to N_{sc}\,. \end{aligned} \tag{40}$$

Notice that these rules are identical to OFC rules with $N_{sc} = 0$ and $\Delta = 4\varepsilon$. This process may lead to a migration avalanche, typical of the lattice models discussed so far. Without interaction, a simple site behaves chaotically. However, by increasing the interaction it reaches a noisy fixed point. Concerning the lattice average, by lowering the threshold level, the collective behavior becomes more pronounced, reflected by the appearance of discrete frequencies on the power spectra; moreover, the time evolution either becomes strictly periodic or it reaches a stable fixed point. Finally, the distribution of avalanche sizes is computed; whereas for a weak interaction the distribution is exponential, for a stronger interaction a power law, characteristic of SOC, was observed.

5. Conclusions

In this paper we have reviewed the collective behavior of a large group of low dimensional systems characterized by two essential features: a dynamical process to update the state of each member of the system and a threshold condition which defines an interactive process between members of the population. The coupling between units is defined in terms of very simple local rules. Within this broad framework we have considered different models ranging from cellular automata where the state of each unit, described in terms of discrete variables, is updated through a random process, to coupled dynamical systems where the internal state is governed by differential equations. In spite of the simplicity of the considered models, the

majority displays a complex behavior. In some cases they settle down in stationary states without characteristic time or length scales typical of self-organized criticality (SOC). In other cases, the attractors are synchronized states with a partial or complete coherence in the temporal activity of the members of a given population. Most interestingly, a few of them display both attractors (and others) depending on the value of the parameters which define the model.

There are several reasons which foster the study of these models. Perhaps, the most relevant is to understand the origin of SOC and identify the underlying mechanisms. Unfortunately, there is no clear answer to this question and the problem remains open. SOC behavior is very sensitive to the action of external factors, it can be destroyed (and created) in many different ways and, *a priori*, it is difficult to find the proper combination of ingredients that may make a system to display it. It is well known that boundary conditions play a relevant role. Big events (avalanches) are usually generated near the boundaries and propagated towards the bulk, but only under suitable conditions which, in general, imply open boundaries. But apart from this important factor, there are other components which also have a crucial effect on the features of the stationary state. For some cellular automata such as the BTW model conservation is the key. For the Zhang model either conservation or a very tiny perturbation of the internal state of the cells. Some continuous driven models display SOC even without conservation such as the OFC model but additionally, in others such as the FF model a dynamical noise is required. In the last two models the role of memory effects (a trace of the initial state) can give the answer.

We have seen that in the continuously driven models the features of the driving are also relevant. The original OFC and the noisy FF models display SOC with constant or quasiconstant driving rate. However, a non-constant driving rate, which implies a convex (concave) relation between the state of each unit and time, leads to new behaviors. In some cases the duality convexity/concavity lead to full synchronization/anti-synchronization (phase locked state where neighbors remain at a fixed phase difference). Then SOC might be understood as an intermediate behavior, balanced between these two extreme situations. In other situations, local synchronization can be responsible for a global SOC behavior. For these reasons, the analysis of systems displaying a rich variety of attractor such as those mentioned in the last section of the paper is of great interest.

Another important feature of the systems considered in this review is the separation of time scales associated with the natural dynamics of each unit and the interaction between them. This separation, quite natural in some situations, seems to be mandatory to observe SOC behavior. If this is true, systems where the transmission of information between neighbors could take a finite time might not display SOC. It would be interesting to pay more attention to this point in the future and see whether it is possible to observe power-law behavior in systems where both time scales are overlapped.

Finally, there are other aspects of interest not sufficiently analyzed so far. The effect of different sources of noise (for instance, the coupling with a thermal bath), the role played by inhibitory rather than excitatory couplings, a careful analysis of the role of memory effects are some of the topics that deserve further research in the future.

Acknowledgments

This work has benefited from discussions with several people, mainly P. Bak, L. F. Abbott, C. Van Vreeswijk, and A. V. M. Herz. Financial support from CICyT, project # PB94-0897, and EC Grant # CHGE-CT92-0009 is also acknowledged. K. C. gratefully appreciates the hospitality of the University of Barcelona.

References

1. B. B. Mandelbrot, *The Fractal Geometry of Nature* (Freeman, San Francisco, 1982).
2. J. Feder, *Fractals* (Plenum Press, New York, 1988).
3. W. H. Press, *Comments Astrophys.* **7**, 103 (1978).
4. P. Dutta and P. M. Horn, *Rev. Mod. Phys.* **53**, 497 (1981).
5. M. B. Weissman, *Rev. Mod. Phys.* **60**, 537 (1988).
6. P. Bak, C. Tang and K. Wiesenfeld, *Phys. Rev. Lett.* **59**, 381 (1987).
7. P. Bak, C. Tang and K. Wiesenfeld, *Phys. Rev.* **A38**, 364 (1988).
8. B. Gutenberg and C. F. Richter, *Bull. Seismol. Soc. Amer.* **34**, 185 (1944).
9. J. M. Carlson and J. S. Langer, *Phys. Rev. Lett.* **62**, 2632 (1989).
10. Z. Olami, H. J. S. Feder and K. Christensen, *Phys. Rev. Lett.* **68**, 1244 (1992).
11. B. Drossel and F. Schwabl, *Phys. Rev. Lett.* **69**, 1629 (1992).
12. P. Bak and K. Sneppen, *Phys. Rev. Lett.* **71**, 4083 (1993).
13. P. Bantay and I. M. Janosi, *Phys. Rev. Lett.* **68**, 2058 (1992).
14. O. Pla and F. Nori, *Phys. Rev. Lett.* **67**, 919 (1991).
15. P. J. Cote and L. V. Meisel, *Phys. Rev. Lett.* **67**, 1334 (1991).
16. J. M. Carlson, J. S. Langer and B. E. Shaw, *Rev. Mod. Phys.* **66**, 657 (1994).
17. P. Bak, K. Chen, J. Scheinkman and M. Woodford, *Ricerche Economiche* **47**, 3 (1993).
18. H. Takayasu, H. Miura, T. Hirabayashi and K. Hamada, *Physica* **A184**, 127 (1992).
19. H. M. Jaeger, C. H. Liu and S. R. Nagel, *Phys. Rev. Lett.* **62**, 40 (1989).
20. P. Evesque, *Phys. Rev.* **A43**, 2720 (1991).
21. M. Bretz, J. B. Cunningham, P. L. Kurczynski and F. Nori, *Phys. Rev. Lett.* **69**, 2431 (1992).
22. E. Morales-Gamboa, J. Lomnitz-Adler, V. Romero-Rochín, R. Chicharro-Serra and R. Peralta-Fabi, *Phys. Rev.* **E47**, R2229 (1993).
23. G. A. Held, D. H. Solina, D. T. Keane, W. J. Haag, P. M. Horn and G. Grinstein, *Phys. Rev. Lett.* **65**, 1120 (1990).
24. S. K. Grumbacher, K. M. McEwen, D. A. Halverson, D. T. Jacobs and J. Lindner, *Am. J. Phys.* **61**, 329 (1993).
25. J. Rosendahl, M. Vekić and J. Kelley, *Phys. Rev.* **E47**, 1401 (1993).
26. J. Rosendahl, M. Vekić and J. E. Rutledge, *Phys. Rev. Lett.* **73**, 537 (1994).
27. V. Frette, K. Christensen, A. Malthe-Sørenssen, J. Feder, T. Jøssang and P. Meakin, *Nature* **379**, 49 (1996).
28. J. Feder, *Fractals* **3**, 431 (1995).
29. D. Dhar, *Physica* **A186**, 82 (1992).

30. C. P. C. Prado and Z. Olami, *Phys. Rev.* **A45**, 665 (1992).
31. A. Mehta and G. C. Barker, *Rep. Prog. Phys.* **57**, 383 (1994).
32. L. Pietronero, P Tartaglia and Y.-C. Zhang, *Physica* **A173**, 22 (1991).
33. D. Dhar, *Phys. Rev. Lett.* **64**, 1613 (1990).
34. S. S. Manna, L. B. Kiss and J. Kertész, *J. Stat. Phys.* **22**, 923 (1990).
35. Y.-C. Zhang, *Phys. Rev. Lett.* **63**, 470 (1989).
36. A. Díaz-Guilera, *Europhys. Lett.* **26**, 177 (1994).
37. A. Vespignani, S. Zapperi and L. Pietronero, *Phys. Rev.* **E51**, 1711 (1995).
38. J. Lomnitz-Adler, L. Knopoff and G. Martínez-Mekler, *Phys. Rev.* **A45**, 2211 (1992).
39. A. Díaz-Guilera, in *3rd Granada Lectures in Computational Physics*, eds. P. L. Garrido and L. Marro, (Springer-Verlag, Berlin, 1995), p. 115.
40. A. Díaz-Guilera, *Fractals* **1**, 963 (1993).
41. E. T. Lu, *Phys. Rev. Lett.* **74**, 2511 (1995).
42. A. Corral and A. Díaz-Guilera, "Symmetries and fixed point stability of stochastic differential equations modeling self-organized criticality", preprint.
43. T. Hwa and M. Kardar, *Phys. Rev. Lett.* **62**, 1813 (1989).
44. G. Grinstein, D.-H. Lee and S. Sachdev, *Phys. Rev. Lett.* **64**, 1927 (1990).
45. T. Hwa and M. Kardar, *Phys. Rev.* **A45**, 7002 (1992).
46. R. Burridge and L. Knopoff, *Bull. Seismol. Soc. Am.* **57**, 3411 (1967).
47. K. Christensen and Z. Olami, *Phys. Rev.* **A46**, 1829 (1992).
48. W. Klein and J. Rundle, *Phys. Rev. Lett.* **71**, 1288 (1993).
49. K. Christensen, *Phys. Rev. Lett.* **71**, 1289 (1993).
50. P. Grassberger, *Phys. Rev.* **E49**, 2436 (1994).
51. K. Christensen, Ph.D. Thesis, University of Aarhus, Denmark, 1992.
52. K. Christensen and Z. Olami, *Phys. Rev.* **E48**, 3361 (1993).
53. A. T. Winfree, *The Geometry of Biological Time* (Springer-Verlag, New York, 1980).
54. J. Buck, *Q. Rev. Biol.* **63**, 265 (1988).
55. H. M. Smith, *Science* **81**, 151 (1935).
56. J. J. Hopfield, *Phys. Today* **47**, 40 (1994).
57. C. Von der Malsburg and W. Schneider, *Biol. Cybern.* **54**, 29 (1986).
58. R. Eckhorn, R. Bauer, W. Jordan, M. Brosch, W. Kruse, M. Munk and H. Reitboeck, *Biol. Cybern.* **60**, 121 (1988).
59. C. M. Gray and W. Singer, *Proc. Natl. Acad. Sci. USA* **86**, 1698 (1989).
60. C. M. Gray, P. Konig, A. K. Engel and W. Singer, *Nature* **388**, 334 (1989).
61. M. Kawato, *J. Math. Biol.* **12**, 13 (1981).
62. N. Ikeda, *Biol. Cybern.* **43**, 157 (1982).
63. C. Torras, *J. Math. Biol.* **24**, 291 (1986).
64. Y. Kuramoto, *Chemical Oscillations, Waves and Turbulence* (Springer-Verlag, Berlin, 1984).
65. Y. Kuramoto, *Prog. Theor. Phys. Suppl.* **79**, 223 (1984).
66. S. Shinomoto and Y. Kuramoto, *Prog. Theor. Phys.* **75**, 1319 (1986).
67. S. H. Strogatz and R. E. Mirollo, *J. Stat. Phys.* **63**, 613 (1991).
68. L. L. Bonilla, J. C. Neu and R. Spigler, *J. Stat. Phys.* **67**, 313 (1992).
69. H. Daido, *Phys. Rev. Lett.* **68**, 1073 (1992).
70. A. Arenas and C. J. Pérez, *Europhys. Lett.* **26**, 79 (1994).
71. H. Daido, *Prog. Theor. Phys.* **88**, 1213 (1992).
72. H. Daido, *Prog. Theor. Phys.* **89**, 929 (1993).
73. H. Sakaguchi, *Prog. Theor. Phys.* **79**, 39 (1988).
74. L. L. Bonilla, C. J. Pérez and J. M. Rubí, *J. Stat. Phys.* **70**, 921 (1993).
75. L. F. Abbott, *J. Phys. A: Math. Gen.* **23**, 3835 (1990).

76. H. G. Schuster and P. Wagner, *Biol. Cybern.* **64**, 77 (1990); *ibid.* **64**, 83 (1990).
77. D. Hansel, G. Mato and C. Meunier, *Concepts Neurosci.* **4**, 193 (1993).
78. A. T. Winfree, *J. Theoret. Biol.* **16**, 15 (1967).
79. G. B. Ermentrout, *J. Math. Biol.* **22**, 1 (1985).
80. R. E. Mirollo and S. H. Strogatz, *SIAM J. Appl. Math.* **50**, 1645 (1990).
81. C. S. Peskin, *Mathematical Aspects of Heart Physiology*, Courant Institute of Mathematical Sciences (New York University, New York, 1975), p. 268.
82. L. Lapicque, *J. Physiol. Pathol. Gen.* **9**, 620 (1907).
83. H. C. Tuckwell, *Introduction to Theoretical Neurobiology* (Cambridge University Press, Cambridge, 1988).
84. S. Bottani, *Phys. Rev. Lett.* **74**, 4189 (1995).
85. Y. Kuramoto, *Physica* **D50**, 15 (1991).
86. C.-C. Chen, *Phys. Rev.* **E49**, 2668 (1994).
87. L. F. Abbott and C. van Vreeswijk, *Phys. Rev.* **E48**, 1483 (1993).
88. A. Treves, *Network* **4**, 259 (1993).
89. M. Tsodyks, I. Mitkov and H. Sompolinsky, *Phys. Rev. Lett.* **71**, 1280 (1993).
90. W. Gerstner, *Phys. Rev.* **E51**, 738 (1995).
91. C. van Vreeswijk, L. F. Abbott and G. B. Ermentrout, *J. Comp. Neur.* **1**, 313 (1994).
92. U. Ernst, K. Pawelzik and T. Geisel, *Phys. Rev. Lett.* **74**, 1570 (1995).
93. X. J. Wang and J. Rinzel, *Neural Comp.* **4**, 84 (1992).
94. A. Corral, C. J. Pérez, A. Díaz-Guilera and A. Arenas, *Phys. Rev. Lett.* **75**, 3697 (1995).
95. H. Sakaguchi, *Prog. Theor. Phys.* **92**, 1039 (1994).
96. Q. Zhilin, H. Gang, M. Benkun and T. Gang, *Phys. Rev.* **E50**, 163 (1994).
97. A. Díaz-Guilera, A. Arenas, A. Corral and C. J. Pérez, "Stability of spatio-temporal structures in a lattice model of pulse-coupled oscillators", preprint.
98. H. J. S. Feder and J. Feder, *Phys. Rev. Lett.* **66**, 2669 (1991).
99. A. A. Middleton and C. Tang, *Phys. Rev. Lett.* **74**, 742 (1995).
100. A. Corral, C. J. Pérez, A. Díaz-Guilera and A. Arenas, in preparation.
101. A. Corral, C. J. Pérez, A. Díaz-Guilera and A. Arenas, *Phys. Rev. Lett.* **74**, 118 (1995).
102. A. V. M. Herz and J. J. Hopfield, *Phys. Rev. Lett.* **75**, 1222 (1995).
103. J. J. Hopfield and A. V. M. Herz, *Proc. Natl. Acad. Sci. USA* **92**, 6655 (1995).
104. J. E. S. Socolar, G. Grinstein and C. Jayaprakash, *Phys. Rev.* **E47**, 2366 (1993).
105. K. Wiesenfeld, J. Theiler and B. McNamara, *Phys. Rev. Lett.* **65**, 949 (1990).
106. M. S. Vieira, *Phys. Rev.* **A46**, 6288 (1992).
107. K. Nagel and H. J. Herrmann, *Physica* **A199**, 254 (1993).
108. I. M. Janosi and J. Kertesz, *Physica* **A200**, 179 (1992).
109. F. Torvund and J. Frøyland, "Strong ordering by non-uniformity of thresholds in a coupled map lattice", *Phys. Scripta* (in press).
110. B. Drossel, *Phys. Rev. Lett.* **76**, 936 (1996).
111. S. Clar, B. Drossel and F. Schwabl, *Phys. Rev. Lett.* **75**, 2722 (1995).
112. A. Csilling, I. M. Janosi, G. Pasztor and I. Scheuring, *Phys. Rev.* **E50**, 1083 (1994).